Modulation of the vertical particle transfer efficiency in the Oxygen Minimum Zone off Peru

Marine Bretagnon[1,2*], Aurélien Paulmier[1], Véronique Garcon[1], Boris Dewitte[1,3,4], Séréna Illig[1, 5], Nathalie Leblond[6], Laurent Coppola[6], Fernando Campos[7,8,9], Federico Velazco[10], Christos Panagiotopoulos[11], Andreas Oschlies[12], J. Martin Hernandez-Ayon[13], Helmut Maske[14], Oscar Vergara[1], Ivonne Montes[8], Philippe Martinez[15], Edgardo Carrasco[10], Jacques Grelet[16], Olivier Desprez-De-Gesincourt[17], Christophe Maes[1,18], Lionel Scouarnec[17]

[1]LEGOS (UPS/CNRS/IRD/CNES), Toulouse, France.
[2]ACRI, Sophia-Antipolis, France.
[3]Centro de Estudios Avanzado en Zonas Áridas (CEAZA), Coquimbo, Chile.
[4]Departamento de Biología, Facultad de Ciencias del Mar, Universidad Católica del Norte, Coquimbo, Chile.
[5]Department of Oceanography, MARE Institute, LMI ICEMASA, University of Cape Town, Cape Town, Rondebosh, South Africa
[6]Sorbonne Université, CNRS, Laboratoire d'Océanographie de Villefanche, LOV, Villefranche-sur-mer, France.
[7]UNAC, Lima, Peru.
[8]IGP, Lima, Peru.
[9]CICESE, Ensenada, Mexico
[10]IMARPE, Callao, Peru.
[11]MIO/CNRS, Marseille, France.
[12]GEOMAR/SFB754, Kiel, Germany.
[13]UABC, Ensenada, Mexico.
[14]CICESE, Ensenada, B.C. Mexico
[15]EPOC, Bordeaux, France.
[16]US IMAGO/IRD, Brest, France.
[17]INSU/CNRS, DT, Brest, France.
[18]LOPS, Brest, France.

Correspondence to: Marine Bretagnon (marine.bretagnon@legos.obs-mip.fr)

Author contributions: M.B., A.P. and V.G. performed the research; A.P. and V.G. designed research; M.B., A.P., V.G., B.D., S.I., F.C., J.M.H-A., O.V., I.M., and P.M. analyzed the data and provided complementary analysis; M.B. and N.L. analyzed the sediment trap samples; A.P., V.G., B.D., N.L., L.C., F.C., F.V., C.P., H.M., E.C., J.G., O.D, A.O., J.M.H-A., O.V., C.M., and L.S. contributed to the sediment trap sampling and analysis as well to the mooring design and implementation; and M.B, A.P., V.G., B.D., C.P, H.M., P.M, and A.O wrote the paper.

Abstract

The fate of the Organic Matter (OM) produced by marine life controls the major biogeochemical cycles of the Earth's system. The OM produced through photosynthesis is either preserved, exported towards sediments or degraded through remineralisation in the water column. The productive Eastern Boundary Upwelling Systems (EBUSs) associated with Oxygen Minimum Zones (OMZs) would be expected to foster OM preservation due to low O_2 conditions. But their intense and diverse microbial activity should enhance OM degradation. To investigate this contradiction, sediment traps were deployed near the oxycline and in the OMZ core on an instrumented moored line off Peru. Data provided high temporal resolution O_2 series characterizing two seasonal steady states at the upper trap: suboxic ($[O_2]$ <25 µmol.kg^{-1}) and hypoxic/oxic (15<$[O_2]$<160

µmol.kg^{-1}) in austral summer and winter/spring, respectively. The OMZ vertical transfer efficiency of Particulate Organic Carbon (POC) between traps (T_{eff}) can be classified into three main ranges (high, intermediate, low). These different T_{eff} ranges suggest that both predominant preservation (high T_{eff} >50%) and remineralisation (intermediate T_{eff} 20<50% or low T_{eff}<6%) configurations can occur. An efficient OMZ vertical transfer (T_{eff}>50%) has been reported in summer and winter associated with extreme limitation in O_2 concentrations or OM quantity for OM degradation. However, higher levels of O_2 or OM, or less refractory OM, at the oxycline, even in a co-limitation context, can decrease the OMZ transfer efficiency to below 50%. This is especially true in summer during intraseasonal wind-driven oxygenation events. In late winter and early spring, high oxygenation conditions together with high fluxes of sinking particles trigger a shutdown of the OMZ transfer (T_{eff}<6%). Transfer efficiency of chemical elements composing the majority of the flux (nitrogen, phosphorus, silica, calcium carbonate) follows the same trend as for carbon, with the lowest transfer level being in late winter and early spring. Regarding particulate isotopes, vertical transfer of $\delta^{15}N$ suggests a complex pattern of ^{15}N impoverishment or enrichment according to T_{eff} modulation. This sensitivity of OM to O_2 fluctuations and particle concentration calls for further investigation into OM and O_2-driven remineralisation processes. This should include consideration of the intermittent behaviour of OMZ with regards to OM in past studies and climate projections.

Introduction

Eastern Boundary Upwelling Systems (EBUSs) are generally known to be highly productive (Chavez and Messié, 2009), associated with significant primary production (479 to 1,213 gC.m^{-2}.yr^{-1}) and elevated concentrations of chlorophyll *a* (1.5 to 4.3 mg.m^{-3}). The high production is caused by prevailing equatorward alongshore coastal winds triggering the dynamic upwelling of cold nutrient-rich waters from the subsurface to the well-lit surface layer. The associated intense biological surface activity produces a large amount of Organic Matter (OM). Part of the OM will sink and be degraded by catabolic processes. Therefore, subsurface OM degradation contributes to the consumption of oxygen (O_2). In conjunction with poor ventilation of the water mass, O_2 consumption leads to the formation of Oxygen Minimum Zones (OMZs), characterized in the global ocean by a suboxic layer between 100 and 1,000 m in depth (Paulmier and Ruiz-Pino, 2009). OM degradation associated with O_2 consumption via respiration or remineralisation may influence biological productivity (fixed nitrogen loss). OM degradation may also influence climate both on short and long timescales (Buesseler et al., 2007; Law et al., 2012; Moffit et al., 2015; Chi Fru et al., 2016) via modulation of the air-sea exchange of climatically-important gases (e.g. CO_2, N_2O and CH_4). Moreover, these impacts on climate and ecosystems may be significant when remineralisation stimulated by high surface productivity takes place in waters that feed the upwelling close to the ocean-atmosphere interface (Helmke et al., 2005; Paulmier et al., 2008). Although poorly documented, the OM fate in OMZ stands out as a major issue, due to O_2 deficiency and its effect on remineralisation processes. Progress will depend on two different hypothesized mechanisms. On one hand, weak oxygenation appears to decrease OM degradation because anaerobic remineralisation is considered to be of an order of magnitude less efficient than aerobic remineralisation (Sun et al., 2002). This low remineralisation efficiency suggests a tendency toward OM preservation and enhanced sediment export. On the other hand, the intense and diverse microbial activity (Devol, 1978; Lipschlutz et al., 1990; Azam et al., 1994; Ramaiah et al., 1996; Lam et al., 2009; Stewart et al., 2012; Roullier et al., 2014) may induce efficient remineralisation and/or respiration. This may particularly be the case in the more oxygenated, warmer upper OMZ layer associated with the oxycline, leading to substantial OM recycling. Remineralisation, involving a relatively variable stoichiometry in the OMZ (Paulmier et al., 2009), depends on several factors. Besides its quantity, OM recycling relies on quality (e.g., lability) and its sinking time through the OMZ layer. The depth of euphotic zone with OM production compared to the depth of oxycline that defines O_2 availability is of particular importance, together with particle size and shape (Paulmier et al., 2006; Stemmann et al., 2004). The conditions that control particle export and remineralisation also affect oxygen distribution and biogeochemical

cycles. A better understanding of the processes that constrain particle export should help to improve estimations of OMZ development and maintenance (Cabré et al., 2015, Oschlies et al., 2017). It is also important to explore the detailed O_2 feedback effect on particles.

The EBUS off Peru is one of the most productive systems, accounting for 10% of the world's fisheries (Pennington et al., 2006; Chavez et al., 2008), with the shallowest oxycline and one of the most intense OMZs (Fig. 1a-b; Paulmier et al., 2009). So, it provides perfect conditions for investigating the relative importance of the aforementioned mechanisms. In order to examine the particle fluxes and their variability, this study focuses on the analysis of a time series compiled from moored sediment traps deployed in the Peruvian OMZ (Fig. 1c). This dataset is part of the AMOP ("Activities of research dedicated to the Minimum of Oxygen in the eastern Pacific", see Methods) project.

Methods

A fixed mooring line was deployed in January 2013 by R/V Meteor ~50 km off Lima at 12°02'S; 77°40'W (Fig. 1). It was recovered in February 2014 by R/V L'Atalante within the framework of the AMOP project ("Activities of research dedicated to the Minimum of Oxygen in the eastern Pacific"; *http://www.legos.obs-mip.fr/recherches/projets-en-cours/amop*). Sediment traps (PPS3 from Technicap Company) were deployed along the line in the oxycline/upper OMZ core (34 m) and in the lower OMZ core (149 m) in order to study particle flux through the water column (Fig. 1c, Fig. 2 & S1; Tab. 1 & S1). The line was also equipped with five sensors measuring pressure, temperature, salinity and oxygen (SMP 37-SBE63), one sensor for fluorescence (ECO FLSB), and four additional temperature sensors (SBE56; Fig 1c). The oxygen sensors have a resolution (smallest change detection) of 0.2 µmol.kg^{-1}, and an initial accuracy and detection limit of 3 µmol.kg^{-1} (Fig. 3, Tab. 2). The resolutions and initial accuracies for the pressure, temperature and salinity sensors (0.2-0.7 and 0.1-0.35 dbar; 0.002 and 0.0001°C; 0.0003 and 0.00001; respectively) induce an estimated resolution and accuracy for density (Fig. 4a-b) of both 0.01 kg.m^{-3} according to the standard TEOS-10 equation. Each sediment trap was equipped with an inclinometer, allowing any incline to be recorded, which is fundamental for data interpretation. Also, to avoid organic matter decay (e.g. grazing) before analysis, the OM was collected in a poisoned solution of sea water with 5% of formaldehyde. The traps sampled particles simultaneously over a period of seven days, during the three months of austral summer ($AMOP_{summer}$ period: January 06 to March 31, 2013). The mooring was serviced in June 2013 and then re-deployed on June 26, 2013; the collection of material in traps resumed on June 28. The sampling interval was extended to eleven days to fit the planned recovery date and to cover a wider period including two seasons (austral winter-spring during $AMOP_{winter\text{-}spring}$). The traps were full on November 06, 2013 but the mooring could not be recovered until February 2014 by R/V L'Atalante. Note that the SMP 37-SBE63 sensors started recording on January 5 at 34 m, on January 7 at 76 m, on January 8 at both 147 and 160 m (Fig. 3), and on June 27, 2013 at 50 m only (due to a technical breakdown).

Before analysing particle samples, we removed the swimmers, which could have actively entered the trap and thus would not represent the strict vertical sinking mass flux. After freeze-drying, the mass flux (dry weight; Fig. S1, Tab. S1) was determined with an accuracy of ±3%. Total carbon (Ctot), particulate organic and isotopic carbon (POC, $\delta^{13}C$) and nitrogen (PON, $\delta^{15}N$) were analysed via an Isotope Resolved Mass Spectrometer (IRMS) Isoprime 100 paired with an Elementary Analyzer (EA) ElementarVarioPyrocube. The carbon and nitrogen content (Fig. 2 & S2, Tab. 3a, S2a-b & S3) was measured with an accuracy of ± 0.2%, and the isotopic $\delta^{13}C$ and $\delta^{15}N$ measurements (Tab. 3c & S4) with an accuracy of ± 0.006 ‰, and0.007 ‰, respectively. Phosphorus and silica (Tab. 3a & S2c-d-S3) were measured by colorimetry, using a spectrophotometer SPECOR 250 plus. Particulate Organic Phosphorus (POP) was analysed using the standard method (Strickland & Parsons, 1972) with an accuracy of ± 3%. The biogenic silica (BSi) was extracted with an alkaline dissolution at

95°C using a kinetic method (DeMaster, 1981) with an accuracy of ± 5%. Ca (for $CaCO_3$ estimation; Tab. S5) was determined from ICP-OES analysis with an accuracy of ± 3%. Systematic replicates for all sediment trap parameters have been analysed to estimate reproducibility, which mainly represents the heterogeneity of the sample. The reproducibility estimated from the Standard Deviation (SD) of the replicates for the total mass fluxes determination (0.12%) is generally lower than the accuracy, except for $\delta^{13}C$.

Daily satellite ASCAT wind measurements (Fig. 4c-d), produced by Remote Sensing Systems (www.remss.com; sponsored by the NASA Ocean Vector Winds Science Team), were used with an accuracy of 2 $m.s^{-1}$. The satellite wind data are consistent with the available in situ wind measurements taken from R/V Meteor during the initial mooring deployment. Wind direction corresponds to alongshore winds favourable to upwelling Ekman transport. The Mixed Layer Depth (MLD; Fig. 4c-d) was estimated from a difference of temperature of 0.5°C following De Boyer Montegut et al. (2004), in phase with the 0.2°C and 0.8°C criteria.

In situ pH_{sw} (Fig. S3) and calcite saturation state ($\Omega_{calcite}$) were calculated with the CO2SYS program (Lewis and Wallace; 1998), using discrete Dissolved Inorganic Carbon measured using a LiCOR 7000 and potentiometric pH_{sw} measurements (25°C). The dissociation constants proposed by Lueker et al. (2002) were used for the calculation with an estimated precision of ± 0.04 units for pH_{sw} in situ, and ± 0.2 units for $\Omega_{calcite}$. Certified reference material (CRM) from Dr. Andrew Dickson's laboratory at Scripps Institution of Oceanography (University of California, San Diego) was used for assessing the precision and accuracy of measurements. The reference material gave a relative difference averaging 2.2 ± 1.1 $\mu mol.kg^{-1}$, with a peak of 4 $\mu mol.kg^{-1}$ (0.2% error) with respect to the certified value.

The analysis accuracy for the sediment trap samples is indicated in Fig. 2. The analysis accuracy has been estimated by propagation of the accuracy of each parameter from a logarithmic expansion for the molar ratios (C:P, N:P, N:P, Si:C, Si:N and Si:P) and all the calculated vertical transfer efficiencies as T_{eff} for POC fluxes (cf. Eq. 1). Standard deviation (SD) between samples representing the variability over the total dataset ($AMOP_{summer}$+$AMOP_{winter\text{-}spring}$) or a given subset of data (e.g. corresponding to high, intermediate or low T_{eff} ranges) has also been indicated in Tables 1, 2, 3 and S1, S2, S3, S4 and S5). The different relative SD present values are higher than the Total Uncertainties (TU = accuracy + reproducibility) for all considered parameters.

Data are available at different time resolutions: 15 min (O_2, density from temperature and salinity); 30 min (fluorescence); 1 day (satellite ASCAT wind); 7 or 11 days for $AMOP_{summer}$ and $AMOP_{winter\text{-}spring}$ datasets, respectively. The sediment trap fluxes include the percentage of Polychaetes relatively to all other collected swimmers, noted %Poly. All fluxes (for the total mass of particles, POC, PON, POP, BSi, $CaCO_3$, $\delta^{13}C$ and $\delta^{15}N$, as well as %Poly), corresponding to a collection period of 7 and 11 days for $AMOP_{summer}$ and $AMOP_{winter\text{-}spring}$ periods, respectively, have been normalized and expressed per day. Hereafter, we will use 7 days as the nominal weekly period. Different averages have been performed to compare with different temporal resolution of other data: from 15 minutes resolution for O_2, density and MLD and from 30 min resolution for the fluorescence to 1 day resolution (Fig. 4); from 15 minutes to 7 (for $AMOP_{summer}$) or 11 (for $AMOP_{winter\text{-}spring}$) days resolution for O_2 (Tab. 2). We verified that different ways to time-average did not modify the main findings of this study. Note however that daily-average MLD (Fig 4c-d) presents a magnitude ~9 times smaller than with the 15min-frequency MLD. This is mainly due to biases induced by the vertical resolution according to the mooring sensor depths. For oxygen, the 1, 7 and 11 day averages have been noted $\overline{[O_2]}_{1day_15min}$, $\overline{[O_2]}_{7days_15min}$ and $\overline{[O_2]}_{11days_15min}$, respectively. $\overline{[O_2]}_{7days_15min}$ and $\overline{[O_2]}_{11days_15min}$ also allow definition of the ratio of POC flux/$[O_2]$, POC flux and $[O_2]$ being at the same temporal resolution (Tab. 2). This ratio corresponds to an availability index in terms of POC flux to be degraded according to the oxygen concentration availability. When the ratio POC Flux/$[O_2]$ reaches extreme values far from the mean range (POC Flux/$[O_2]$>Average+SD or POC Flux/$[O_2]$<Average-SD),

we define a severe limitation by oxygen only or by OM only, respectively. When this ratio POC Flux/[O_2] is within the interval [average –SD, average +SD], we define a co-limitation with either O_2 or OM as the main factor limiting OM degradation.
Sediment trap fluxes, O_2 concentrations and other quantities considered in this study (e.g. the ratio of POC flux/[O_2]) have been averaged on the different T_{eff} ranges (Tab. 1-3 & S1-S5).

RESULTS AND DISCUSSION

Particle transfer efficiency through the OMZ

a) Temporal modulation of particles and POC fluxes and their transfer efficiencies

The transfer of particles through the Peruvian OMZ is studied using data collected at the two fixed sediment traps, one located in the oxycline/upper core (34 m) and the second in the lower core (149 m). Seasonally, at 34 m, the mass fluxes during summer are about 60% lower than during winter-spring ($AMOP_{winter\text{-}spring}$: 986 $mg.m^{-2}.d^{-1}$ on average; cf. Fig. S1, Tab. S1). At 149 m, the mass fluxes during summer are about 80% higher than during winter-spring ($AMOP_{winter\text{-}spring}$: 95 $mg.m^{-2}.d^{-1}$ on average; cf. Fig. S1, Tab. S1). Intra-seasonally, during summer ($AMOP_{summer}$), the variability of fluxes at 34 m and 149 m is 3 times and 40% lower than during winter-spring ($AMOP_{winter\text{-}spring}$; cf. Tab. S1) with SD = 144% (39<4647 $mg.m^{-2}.d^{-1}$) and 138% (12<488 $mg.m^{-2}.d^{-1}$), respectively.
The POC flux (Tab. 1) is globally proportional to the total particle flux (R^2 = 0.92) (Fig. S2a). Therefore analysis of the total particle flux and the POC flux will lead to similar results. To investigate the influence of the oxygen-deficient layer between both traps for each season, we use the POC transfer efficiency (T_{eff}) introduced by Buesseler et al. (2007), and defined as:

$$Teff = \frac{POC_{149}}{POC_{34}} \times 100 \quad (1)$$

The transfer efficiency allows determination of the ability of the system to preserve organic matter quantity and to foster the export of carbon from the productive layer. The higher the transfer efficiency, the higher the proportion of particles reaching the deeper trap. Therefore, T_{eff} is an index of the relative amount of carbon which reaches the deeper trap.
The mean transfer efficiency appears to be relatively similar for both datasets (T_{eff} ~45%). However, T_{eff} values present a strong temporal variability, with T_{eff} more than 3 times more variable for $AMOP_{winter\text{-}spring}$ than for $AMOP_{summer}$ (Fig. 2; Tab. 1).

T_{eff} can be higher than 100%, referring to particle accumulation between both traps. T_{eff}>100% is potentially attributable to advection of particles or to primary or secondary production between traps. T_{eff} is never higher than 100% during $AMOP_{summer}$ but it is 3 times higher during $AMOP_{winter\text{-}spring}$ ($AMOP_{winter\text{-}spring}$-S1, -S3, -S6; T_{eff} = 135, 106 and 149%, respectively). Due to the potential bias affecting these values without considering the OMZ influence, T_{eff} > 100% were discarded. Excluding these very high T_{eff} results, transfer efficiency varies between 1 and 71%. Three ranges of variation can be defined: high, intermediate and low. The high range with relatively efficient transfer (T_{eff}>50%) corresponds to a predominance of OM preservation. This preservation is observed for a third of the total samples, namely the first 3 samples of $AMOP_{summer}$ ($AMOP_{summer}$-S1, -S2 & -S3), the sample between 17 and 24 March ($AMOP_{summer}$-S11) and two samples in winter ($AMOP_{winter\text{-}spring}$-S2 & -S5). Conversely, the other samples correspond to a predominance of potential OM degradation or remineralisation. In late winter/early spring, the proportion of particles reaching the deeper trap is very low (low range of T_{eff} < 6%). This period represents half of the $AMOP_{winter\text{-}spring}$ period (from September 2 to November 6) and seems to correspond to the main period of OM degradation. Between these extreme high and low values, T_{eff} presents an intermediate range between 20 and 50%. Intermediate T_{eff} occurs mainly in summer from January 27 to March 31 ($AMOP_{summer}$-S4, -S5,-S6, -S7, -S8, -S9, -S10 and –S12). Within the 20<50% T_{eff} range, the six samples in summer ($AMOP_{summer}$-S4, -S6, -S8, -S9, -S10 and -S12), and one sample in winter ($AMOP_{winter\text{-}spring}$-S4) present a low intermediate T_{eff} range of 20<38%. The definition of these three main ranges of the transfer efficiency

(low, intermediate, high) appears to be consistent since each one presents a slight variation with SD of: 7% for T_{eff} <6%; 7% for 20<T_{eff}<50%; 1% for T_{eff}>50%.

Note that the vertical profile of POC flux is assumed to follow a power law (Suess, 1980; Martin et al., 1987).

$$Flux_{149} = Flux_{34} * \left(\frac{149}{34}\right)^{-b} \quad (2)$$

The *b* coefficient represents the attenuation of the curve and therefore an index for OM respiration during sinking. Fitting *b* on the AMOP dataset reveals temporally-varying *b* values (between 0.23. and 2.97, Tab. 1). Small and large *b* values indicate a slow or rapid OM decay, respectively. Even if this transfer layer (between both traps) is relatively shallow and covers a short distance (115 m) compared to other studies (e.g., between 200 and 1,000 m, Devol and Hartnett, 2001; Miquel et al., 2011; Heimburger et al., 2013), *b* values are in the same range as previous estimates. The largest b values are estimated from September 2 ($AMOP_{winter-spring}$-S7) to November 6 ($AMOP_{winter-spring}$-S12) with a maximum of 2.97 on September 13 ($AMOP_{winter-spring}$-S8). These high values correspond to the minimal transfer efficiency (low range of T_{eff}<6%) and are consistent with Martin's values observed for the oxygenated North Pacific (0.90 ± 0.06). The lower *b* values (between 0.23 and 0.98, Tab. 1) are in line with those generally observed in the Equatorial Pacific OMZ (between 0.63 and 0.9: Berelson, 2001), in the Mexican OMZ (about 0.36 : Devol and Hartnett, 2001), in the Peruvian OMZ (0.66 ± 0.24: Martin et al., 1987) and in the Arabian Sea OMZ (0.22: Roullier et al., 2014; 0.59 ± 0.24: Keil, 2016). The temporal modulation of *b* is comparable to the one associated with the spatial switch from the coast to the open ocean off Peru (Packard et al., 2015) as well as from high to low latitude regions (Marsay et al., 2015). Globally, and in line with the transfer efficiency, the strongest attenuation was observed in spring (*b* = 2.43 ± 15%) and the weakest in winter (*b* = 0.47 ± 57%). One can notice that the attenuation is also 4 times stronger and 2.5 times more variable in spring than in summer, where *b* is on average 0.62 ± 39%. Considering the ranges previously defined, *b* = 2.43 (±0.37) for low T_{eff} (<6%), *b* = 0.74 (± 0.15) for intermediate T_{eff} (20< 50%) and *b* = 0.36 (±0.06) for high T_{eff} (>50%).

b) Significance of transfer efficiency

While the transfer efficiency (T_{eff}) between the upper (34 m) and lower (149 m) sediment traps allows a mathematical distinction between ranges of POC export efficiency, it is crucial to investigate the physical significance of this T_{eff}. Particles sampled at 149 m are not necessarily associated with the same vertical flux as those previously sampled at 34 m over the 7 or 11-day period. This is due to the following three main processes: a) horizontal transport, b) vertical sinking speed defining the finite time between both traps and c) particle production between both traps involving different trophic levels.

T_{eff} may be affected by horizontal advection of particles as well as by sediment trap line inclination, in response to the coastal current system (e.g., shear due to the northward flow at the surface and southward flow in the subsurface layers). These typical methodological biases in sediment trap studies are known to potentially affect the collection of particles and its efficiency. Here, the mean alongshore (poleward) current reaches ~12 $cm.s^{-1}$ (slower than 15 $cm.s^{-1}$) over the duration of the experiment in the vicinity of the sediment traps. This is based on in situ data (AMOP cruise), climatology (Chaigneau et al., 2013) and estimates from climatological regional model simulations (Montes et al., 2010; Dewitte et al., 2012). Therefore, the collection of particles is considered to be marginally affected by currents in this transfer layer (Baker et al., 1988). This is confirmed by a small inclination of the mooring line (<5°). However, the only three samples presenting values of T_{eff}>100% ($AMOP_{winter-spring}$-S1, -S3 and -S6) are characterized by a relatively high inclination anomaly (related to the mean inclination) of the mooring line. This high inclination anomaly can be assigned to a significant modification of the horizontal currents mean state. Zonal advection of particles from a more productive region in the lower trap could explain anomalous high transfer.

Vertically, we assume that upwelling or downwelling events (velocity below 0.5 $m.d^{-1}$) do not significantly impact particle sinking speed (ranging from 1 to 2,700 $m.d^{-1}$; Siegel et al., 1990; Waniek et al., 2000). In addition, the quantity of matter collected by the sediment trap in each cup at 149 m may be different to that collected in the corresponding cup at 34 m. This depends on the vertical velocity of specific particles. Particle velocity also determines exposure time to degradation activity in the water column. Therefore, the probability of particle degradation may increase for slower (generally smaller) particles. They spend a longer time in the subsurface active remineralisation layer between 34 and 149 m, which could be the case for samples with T_{eff}<50%. Conversely, the large amount of matter collected at 149 m for the high T_{eff} range (>50%) might be explained by the presence of potentially less-degraded particles, resulting from a faster sinking velocity (McDonnell et al., 2015). In theory, the sinking velocities of biogenic particles depend on the three-dimensional properties of the flow field as well as on various intrinsic factors (such as their sizes, shapes, densities, porosities; Stemmann and Boss, 2012). These intrinsic factors can be modified along their fall by complex bio-physical processes (e.g. aggregation, ballasting, and trimming by remineralisation). Note that processes like aggregation (e.g. flocculation) or disaggregation may affect the vertical transfer, as they modulate the sinking rate. Indeed, while disaggregation transforms fast-sinking large particles into small suspended particles, aggregation of small particles will induce their sinking. However, the samples from the present study are mainly composed of faecal pellets, and in a relatively equal proportion for both traps. Therefore, bio-physical processes do not appear to be the main factor which modulates transfer efficiency.

Finally, subsurface particle production between 34 and 149 m can affect T_{eff}. For instance, T_{eff} can be affected by the presence of a deep or Secondary Chlorophyll Maximum (SCM), which can sometimes be more intense than the primary maximum in OMZ areas (Garcia-Robledo et al., 2017). The fluorometer data at 31 m suggest an intermittent increase in fluorescence around this depth (Fig. 4e-f). However, the high fluorescence values could be attributable to the detection of an SCM or to deepening of the surface mixed layer, mixing the surface chlorophyll with the subsurface layer. To complement fluorescence data, $\delta^{13}C$ values (Tab. S4) provide some information about particle production and typical processes linked to surface productivity. Here, the transfer efficiency of $\delta^{13}C$ is roughly constant (between 88% and 105%, Tab. S4). This suggests no significant primary production below the top trap and therefore no significant contribution of an SCM. In addition, the water column between 34 m and 149 m is mostly below the euphotic layer where primary producers are mainly active. Thus, particle production is considered to be related to higher trophic levels only, in particular zooplankton (e.g. detritus due to excretion and mortality). Zooplankton can also induce active vertical transport of particles not directly considered here. However, zooplankton production should be pointed out for $AMOP_{summer}$-S1. $AMOP_{summer}$-S1 is characterized by an oxygen event (>10 $\mu mol.kg^{-1}$, Fig. 4a) but with an unexpectedly high T_{eff} (71%) suggesting preferential OM preservation. This sample is different from the others previously mentioned, the number of swimmers collected being 3 times higher than the average of the $AMOP_{summer}$ dataset, especially in the lower trap. This $AMOP_{summer}$-S1 specificity is raising the influence of the active transfer between both traps and potentially secondary production.

In this study, we assume that a) similar particles are collected in the upper and lower traps for each sampling period; b) all particles collected in the deep trap are, for each sampling period, subject to a comparable time in the OMZ layer. Note that all the $AMOP_{summer}$ samples in summer and the first six $AMOP_{winter\text{-}spring}$ samples (from $AMOP_{winter\text{-}spring}$-S1 to –S6) in winter appear to be subject to a comparable trophic level effect. Indeed, samples are composed of around 60-70% faecal pellets, therefore spending a similar amount of time in the OMZ. However, for the six last $AMOP_{winter\text{-}spring}$ samples (from $AMOP_{winter\text{-}spring}$-S7 to –S12) in late winter/early spring, the proportion of faecal pellets and marine snow inverts. For $AMOP_{winter\text{-}spring}$ dataset, low T_{eff} (from $AMOP_{winter\text{-}spring}$-S7 to –S12) can be explained by the higher proportion of small particles (as marine snow), which is potentially easily degradable.

Transfer efficiency (T_{eff}) is controlled by the degradation of particles occurring below the productive layer. Organic matter degradation can be due to macro-organisms feeding (Lampitt et al., 1990) or to microbial activity (e.g. Devol, 1970; Lam et al., 2009; Stewart et al., 2012 and Roullier et al., 2014). This degradation implies a dependence on oxygen availability. Low oxygen availability could constrain zooplankton in a specific layer, therefore limiting feeding. Low oxygen availability could also reduce the microbial activity. Aerobe remineralisation is considered to be 10 times more efficient than anaerobe remineralisation (Sun et al., 2002; Taylor et al., 2009). However, in addition to the main requirement of catabolic energy fuelled by O_2 availability, OM bioavailability should feed the substrate anabolic requirement of the heterotrophic microbial community controlling remineralisation activity. This argument is in line with previous studies showing microbial nitrogen cycling regulated by OM export (Kalvelage et al., 2013). Therefore, for intermediate ($20<T_{eff}<50\%$) and high T_{eff} (>50%), OM degradation is considered as limited, whereas for low T_{eff} (< 6%) it is not. The role of oxygenation and OM availability in OM degradation was explored. This was to provide a better estimation of whether the quantity of carbon remains available for surface production and air-sea exchange, or whether it is preserved and exported toward the sediment.

Key parameters modulating particle transfer efficiency

The respective roles of oxygen and organic matter in modulating transfer efficiency will be evaluated.

a) The role of oxygen

Transfer efficiency (T_{eff}) shows a variation between seasons, as well as at an intraseasonal level. The role of oxygen is investigated by considering temporal changes in oxygenation and whether they could be a potential factor associated with changes in remineralisation activity. Could this explain the T_{eff} modulation?

Vertical and temporal [O_2] changes mainly occur near the oxycline and upper OMZ core (upper trap) rather than in the lower OMZ (lower trap). In the lower OMZ, O_2 concentration remains stable, reaching the lowest detection limit (Fig. 3). Close to the upper trap, oxygen concentration can then be a key-factor triggering limitation of remineralisation.

Seasonally, mean oxygen concentration appears to be ~10 times lower for $AMOP_{summer}$ (~5 µmol.kg^{-1}) than for $AMOP_{winter\text{-}spring}$ (~60 µmol.kg^{-1}; Fig. 4a-b). The daily-averaged oxygen concentration at 34 m highlights the existence of two steady states regarding oxygenation: i) the suboxic conditions occurring in summer, where [O_2] stays below 25 µmol.kg^{-1}, and/or with a shallower oxycline; ii) the hypoxic/oxic conditions occurring in winter and early spring, where [O_2] is always above 15 µmol.kg^{-1}, and/or with a deeper oxycline (Fig. 4a-b). Suboxia corresponds to limiting conditions for both aerobe micro- and macro-biological (e.g. bacteria and zooplankton) OM degradation thereby impacting the vertical transfer efficiency (T_{eff}). This is confirmed by the fact that the abundance of swimmers during $AMOP_{summer}$ is half the amount as during $AMOP_{winter\text{-}spring}$. This is also confirmed by the relative abundance of polychaetes, known to better tolerate suboxic conditions than copepods. The number of reported polychaetes is 22 times higher at the oxycline during $AMOP_{summer}$ than during $AMOP_{winter\text{-}spring}$ (Tab. 2). Oxygen concentration may also indirectly impact T_{eff}. More oxygenated conditions (e.g. during $AMOP_{winter\text{-}spring}$) allow copepods, for instance, to colonize depths between both traps, and therefore potentially produce particles within this layer through sloppy feeding, faecal pellets and carcasses sinking. The latter mechanism may explain the higher than 100% T_{eff}.

In addition to concentration considerations, [O_2] for $AMOP_{summer}$ is 10 times less variable (SD= 2.6 µmol.kg^{-1} for $\overline{[O_2]}_{7days_15min}$) than for $AMOP_{winter\text{-}spring}$ (SD=28 µmol.kg^{-1} for $\overline{[O_2]}_{11days_15min}$; Tab. 2). This difference regarding variability highlights less intense and 2 times less frequent oxygenation events during $AMOP_{summer}$ than during $AMOP_{winter\text{-}spring}$ (Fig. 4a-b). The more elevated O_2-conditions observed during $AMOP_{winter\text{-}spring}$ are favourable to OM degradation through both micro- and

macro-organisms. This is therefore consistent with a lower T_{eff} (<6%), where no limitation of the degradation mechanisms is considered.

Intra-seasonally, for $AMOP_{summer}$ associated with an O_2 limitation period, specific relative and significant oxygenation conditions ($5.5 \leq 12.5$ µmol.kg^{-1}) can be identified according to the weekly averages. These oxygenation conditions, 30% higher than the seasonal mean O_2 steady state, occur between January 6 and 13 ($AMOP_{summer}$-S1); January 27 and February 3 ($AMOP_{summer}$-S4); February 10 and 17 ($AMOP_{summer}$-S6); February 24 and March 17 ($AMOP_{summer}$-S8, -S9, -S10; Tab. 2, Fig. 4a). In such cases, aerobe remineralisation could still be active and potentially coupled with underlying anaerobe remineralisation. This coupling could lead to relatively more efficient OM degradation (Sun et al., 2002), consistent with relatively low T_{eff} ($24 \leq 38$%; Tab. 1), except for $AMOP_{summer}$-S1 (considered apart; cf section *Significance of transfer efficiency*). In contrast, less oxygenated conditions ($3.5 \leq 4.9$ µmol.kg^{-1}) inducing potential O_2 limitation are consistent with relatively higher intermediate T_{eff} ($38 \leq 57$% for $AMOP_{summer}$-S2, -S3, -S5, -S7, -S11, -S12). In these cases, a severe O_2 limitation can be considered, as the oxygen concentration appears to be about 25% lower than the seasonal mean O_2 steady state. This severe O_2 limitation covered situations considered limited by O_2 only (POC flux/$[O_2]$>Average+SD meaning >17+10: $AMOP_{summer}$-S2&3) but also by OM only (POC flux/$[O_2]$<Average-SD, meaning <17-10: $AMOP_{summer}$-S11).

At higher frequency, within the weekly period, the oxygenated conditions present oxygenation episodic events with: i) a higher daily occurrence (≥2 per week; up to 6 events for $AMOP_{summer}$-S8); ii) often relatively intense ($\overline{[O_2]}_{1day_15min}$,reaching 24.2 µmol.kg^{-1} for $AMOP_{summer}$-S9; Fig. 4a). In contrast, the less oxygenated conditions present only low occurring oxygenation events (≤2 per week), which are generally less intense.

The oxygenation events, reported for both $AMOP_{summer}$ and $AMOP_{winter\text{-}spring}$, are linked with density minima (<26.1 kg.m^{-3}) and are relatively consistent with a deepening of the Mixed Layer Depth (MLD). This suggests vertical diapycnal mixing with surface water (Fig. 4a-b-c-d). Induced vertical mixing appears to be driven by an increase in wind intensity, frequency (more than one wind pulse per week) and duration (~10 days). Globally, the averaged density for $AMOP_{winter\text{-}spring}$ is lighter than $AMOP_{summer}$ by ~0.07 kg.m^{-3}. Short wind-driven mixing events are followed by a longer re-stratification period associated with an $[O_2]$ decrease (of ~5 µmol.kg^{-1} for $AMOP_{summer}$ and >20 µmol.kg^{-1} up to 100 µmol.kg^{-1} for $AMOP_{winter\text{-}spring}$) and density increase (of >0.1 kg.m^{-3}, up to 0.4 kg.m^{-3} for AMOP 2), then stabilization. The sequences of mixing/stratification and oxygenation/deoxygenation could have been induced by sequences of stirring (or downwelling/upwelling). These sequences are typically observed during upward transportation of deeper, denser and lower $[O_2]$ water, in response to a modulation in alongshore winds favourable to Ekman transport. A propagation of coastal trapped waves, with in-phase vertical fluctuations in the density and oxygen isopleths, can also take place (Sobarzo et al., 2007; Dewitte et al., 2011 and Illig et al., 2014). These wind-driven oxygenation events during the lowest seasonal steady state oxygenation as in $AMOP_{summer}$, potentially modulate the intensity of remineralisation at an intra-monthly frequency. In fact, during summer, transfer efficiency varies up to a factor of 2 (24<57%) associated with oxygenation events. These oxygenation events allowing less O_2 limitation, are consistent with a relatively lower intermediate T_{eff} between 20% and 40% (e.g. for $AMOP_{summer}$-S4, -S6, -S8, -S9 and -S10).

The transfer efficiency (T_{eff}) decreases from high (>50%) to low intermediate (20<38%) when $[O_2]$ at the oxycline, or in the upper OMZ, increases during oxygenation events. This T_{eff} decrease occurs at: i) a seasonal scale from the limit of detection of $\overline{[O_2]}_{1day_15min}$ ~5 µmol.kg^{-1} up to ~25 µmol.kg^{-1} in summer; ii) an intraseasonal scale from less (~5 µmol.kg^{-1} in summer) to more (~60 µmol.kg^{-1} in winter/spring) oxygenated mean states. However, for the similar winter/spring hypoxic/oxic conditions at the oxycline, the modulation of T_{eff} (between 1% and 68%) suggests that a factor other than oxygen is restricting the mechanism of OM degradation and remineralisation.

b) The role of Organic Matter

In addition to oxygen, transport mechanisms, sinking time and trophic transfer having an effect, other processes which depend on the nature of particles may explain the contrast in transfer efficiency (T_{eff}). Collected particles are marine and organic. Collected particles can mainly be considered as OM, based on the similar modulation of T_{eff} for POC and the transfer efficiency for the total particles (Fig. S1, S2 and S4). Indeed C:N ratios at 34 m (between 5.7 and 10.1, Tab. 3b and S3a) are always below 20, which is characteristic of a marine origin (Mayers, 1993), although approximately 13% higher than the canonical Redfield values (Redfield et al., 1963). Carbon isotopic signatures ($\delta^{13}C$) are between -22.7 and -17.4‰ and $\delta^{15}N$ between 3.5 and 13.1‰ (Tab. 3c and S4). These $\delta^{13}C$ values are consistent with marine organic compounds, and inconsistent with terrigenous influence (Degens et al., 1968; Ohkouchi et al., 2015; Bardhan et al., 2015).

Variability in the exported OM acts as anabolic biogeochemical forcing, supplying the OMZ with particles to be degraded and remineralised. OM variability is thereby potentially mitigating the transfer efficiency (T_{eff}). The variability of the particle flux collected in the upper trap is thus considered in order to understand the role of OM quantity and quality on transfer efficiency (T_{eff}).

Quantitatively, the POC flux at 34 m presents a seasonal variability. POC flux values are 40% higher during $AMOP_{winter\text{-}spring}$ than $AMOP_{summer}$ (on average 131 and 93 $mgC.m^{-2}.d^{-1}$, respectively). POC flux also presents a stronger intra-seasonal variability during $AMOP_{winter\text{-}spring}$, being more than 1.5 times more variable than during $AMOP_{summer}$. This is confirmed by the fluorescence measurement at 31 m, higher for $AMOP_{winter\text{-}spring}$ than for $AMOP_{summer}$ (Fig. 4e-f). In fact, a deepening of the MLD as a response to the wind strengthening can increase the fluorescence values at 31 m by stronger vertical mixing of the chlorophyll produced at the surface. Thus, mixing of the surface productivity with the subsurface layers could contribute to an increase of fluorescence in the subsurface.

During the $AMOP_{winter\text{-}spring}$ winter period, low light availability and high mixing (Fig. 4d) induce low surface productivity according to lower fluorescence values at 31 m. The lower fluorescence contributes to the low POC flux recorded by the upper trap (Fig. 4f). Conversely in spring, the water column is stratifying (MLD decrease; Fig. 4d). The surface productivity increases in line with higher fluorescence values (globally higher than $1\mu g.l^{-1}$). This productivity increase leads to a higher concentration of particles and a POC flux about 10 times stronger than in winter (239.58>24.79 $mgC.m^{-2}.d^{-1}$; Fig. 2b&4f). The T_{eff} decrease from winter to early spring, characterised by high and intermediate (>20%) and low (< 6%) values, respectively, follows a power tendency line (Fig. 5). An increase in remineralisation activity as a consequence of a primary productivity increase could be suspected, as previously reported for the anoxic basin of Cariaco (Thunell et al., 2000).

During $AMOP_{summer}$ in suboxic conditions at the oxycline and O_2 limitation of OM degradation, the events of slight oxygenation have supported the modulation of T_{eff} from high (>40%; $AMOP_{summer}$-S2, -S3, -S5, -S7, -S11) to low (<40%; $AMOP_{summer}$-S6, -S8, -S9, -S10) intermediate values, except for $AMOP_{summer}$-S1 (considered apart; cf. section *Significance of transfer efficiency*). Now, the variability in OM quantity together with O_2 availability is analysed to identify conditions potentially leading to remineralisation-like and preservation-like configurations (T_{eff} below or above 50%). The highest POC fluxes (>85 $mgC.m^{-2}.d^{-1}$) at 34 m occur from $AMOP_{summer}$-S1 to -S6 and $AMOP_{summer}$-S8 to -S9 (Fig. 2a&4e). For $AMOP_{summer}$-S7 and from $AMOP_{summer}$-S10 to -S12, POC fluxes are ~30% lower than the seasonal average. The low OM quantity could therefore explain a weaker remineralisation, and thus a slightly higher T_{eff} (up to 57%). However, limitation of both O_2 and OM, simultaneously (co-limitation) or not, should be considered. When the ratio POC Flux/$[O_2]$ is far from the mean range, POC Flux/$[O_2]$ values define a severe limitation in OM only (<7 for $AMOP_{summer}$-S11) or O_2 only (>27 for $AMOP_{summer}$-S2&3). In these cases, T_{eff} becomes

high. Conversely, the ratio POC Flux/[O_2] remains closer to the mean range (7<27) for $AMOP_{summer}$-S4, -S5, -S6, -S7, -S8, -S9, -S10 & -S12, except for $AMOP_{summer}$-S1 (considered apart; cf. section *Significance of transfer efficiency*). In these cases, T_{eff} remains intermediate (20<50%) associated with a potentially balanced co-limitation in O_2 and OM on OM degradation.

Qualitatively, the evolution of elemental fluxes at 34 m should be considered in investigating whether the composition of a more or less labile OM can affect transfer efficiency (T_{eff}) in addition to the OM availability. Interpretation of organic matter quality changes over the short depth interval of 115 m can only provide limited insights, especially as there are no information on processes occurring over this depth interval at any stage of the deployment. For both datasets, POC and PON fluxes show a strong linear correlation with the total particle mass fluxes at the upper trap as well as for the lower trap (R^2 = 0.98 for both traps Fig. S2a, b).

To study the influence of particle quality on transfer efficiency, the composition was averaged for the three main ranges of T_{eff}. Also, as the matter collected in the trap is mainly organic, only the four main components (POC, PON, POP and BSi) were considered here. Whatever the range of T_{eff}, the particle flux is dominated by POC. Then, BSi, PON and POP contribute in different proportions to the particle flux (Fig. 6b; Tab. 3a&S2). For low T_{eff}, POC dominates with only 49%. For intermediate (including $AMOP_{winter-spring}$-S4) and high T_{eff} ranges, POC remains relatively constant reaching 65-66% of the total POC+BSi+PON+POP. On the contrary, BSi reaches 43% for low T_{eff}. For the relatively constant intermediate and high T_{eff} ranges, BSi only reaches 25%. Whatever the T_{eff} range, PON and POP have a relatively stable contribution of 7-8% and 1-2%, respectively. Between intermediate and high T_{eff} ranges, the relative constancy in the composition of the particles does not allow the investigation of the influence of the quality on transfer efficiency.

Nevertheless, for the remineralisation event observed in $AMOP_{winter-spring}$-S4, while OM quantity was expected to limit remineralisation, the influence of quality should be pointed out as another factor acting on its low intermediate T_{eff} (32%; Fig. 6, Tab. 1). Indeed, this sample is specifically characterized by a relatively low BSi content (~ 19%, 50% lower than the winter average) and the highest PON and POP proportions (35% and 5 times higher than the winter average, respectively, Fig. 6b; Tab. S2). For this sample, the relative proportion of BSi decreases and the one of PON increases as compared to the other intermediate, low and high T_{eff} samples, leading to less refractory and more labile matter, preferentially degraded. The difference in composition for this sample could also be seen in terms of calcium carbonate. $AMOP_{winter-spring}$-S4 $CaCO_3$ upper flux exhibits a maximum at this date compared to other intermediate and high T_{eff} (Tab. 3c) and about 5 times higher (20% of the total mass flux) than the average for the entire dataset (Tab. S5). A difference in the phytoplankton community could be at the origin of this distinction. Indeed, at the beginning of the $AMOP_{winter-spring}$ dataset and up to this sample, the MLD is relatively stable. No strong MLD deepening is observed as a consequence of wind intensification. As the surface productivity is mainly due to diatoms, this long period with no strong mixing events can induce silica depletion at the surface, limiting diatom growth. This hypothesis is supported by the analysis of the phytoplankton functional types around the mooring location using MODIS data and the algorithm developed by Hirata et al. (2011). For $AMOP_{winter-spring}$-S4, prymnesiophytes become the most influent phytoplanktonic group. The dominance of prymnesiophytes in this sample could have induced a change in the composition of the sinking particles. In particular, their BSi proportion decreases, leading to a more labile matter.

The composition of the matter at the upper trap can also be observed as a function of the particulate molar ratios to identify the relative elemental excess or deficit. Whatever the considered range of T_{eff}, biogenic silica appears to be in excess. Si:C, Si:N and Si:P are on average 3.9, 4.4 and 3.0 times higher than the classical ones, respectively (Tab. S3b). The strongest BSi excess can be assessed for low T_{eff} (ratio ~5 times higher than the classical ones; Tab. 3b). For the other elemental ratios, low T_{eff} appears to be different from the other T_{eff} ranges. Indeed, low T_{eff} presents a relative POP deficit (C:P and N:P ~20% higher than classical

ones) with a C:N ratio equal to classical one (6.67). On the contrary, the other T_{eff} ranges present a relative POP excess (C:P and N:P about half the amount of classical ones), with a PON deficit relative to POC (C:N) between 12 and 24%.

Molar ratios at 34 m for $AMOP_{winter\text{-}spring}$-S4 confirm the analysis of elemental composition (Fig. 6b). In particular, BSi deficit (e.g. Si:C and Si:N about twice as low and Si:P ~4 times lower than classical ones) and P excess (C:P and N:P ~8 times higher than classical ones; Tab. S3) are reported. However, Si:P, C:N, C:P and N:P present strong intra-seasonal variability. Relative SD reaches 60% for the intermediate T_{eff} range. In particular, reported Si:P, C:N, C:P and N:P values are below or above standard reference levels, whatever the T_{eff} range.

Therefore, the OM quantity produced above the oxycline appears to have a stronger influence on transfer efficiency than the OM quality of the sinking particles. However, more or less labile materials can also contribute to better preservation and export of particles towards sediment or their remineralisation in the upper layers of the ocean. Together with oxygenation conditions, OM quantity is a major factor in triggering strong remineralisation. It may be strengthened or mitigated by OM quality, which is considered here as a secondary factor. The significance of co-factors is consistent with the fact that oxic or anoxic conditions have a different effect on OM degradation (faster or slower, respectively) depending on the OM components considered (e.g. Taylor et al., 2009).

Vertical flux modulation for elemental and isotopic components

The analysis of particle transfer efficiency through the OMZ has been focussed on the carbon element, defining three main T_{eff} ranges. Here we study the transfer efficiencies of other particle components (T_{effPON} for PON, T_{effPOP} for POP, T_{effBSi} for BSi, $T_{effCaCO3}$ for $CaCO_3$, T_{eff13C} and T_{eff15N} for isotopic signatures) as well as their modulation and distribution.

All transfer efficiencies for the elemental composition present a low range (<15%), clearly dissociated from the intermediate (15<55%) and high (55<80%) ranges (Tab.S2). T_{effPOP} alone shows a more gradual transition between 0 and 55%. Due to the similar distribution of the transfer efficiency ranges for POC and other elemental components, the three main T_{eff} ranges (low, intermediate, high) defined for T_{eff} are kept (Fig. 7; Tab. 3). However, at low T_{eff}, T_{effPOP} remains higher than 6% (15%). T_{effPOP} of 15% represents a decrease with respect to the intermediate range and is five times lower than for the other elements. This could indicate a relative accumulation of phosphorus. In remineralisation-like configuration, potential accumulation suggests that phosphorus material may remain more refractory than nitrogen-rich amino-acids which are preferentially degraded (Van Mooy et al., 2002; Böning et al., 2004; Pantoja et al., 2004; Diaz et al., 2008). Considering the fluxes of one element relatively to the other, the study of the vertical transfer efficiency of the elemental ratios ($T_{effC:N}$ for C:N, $T_{effC:P}$ for C:P, $T_{effN:P}$ for N:P, $T_{effSi:C}$ for Si:C, $T_{effSi:N}$ for Si:N and $T_{effSi:P}$ for Si:P; Tab. 3b&S3) supports the previous analysis (from Fig. 7). The vertical transfer efficiency $T_{effC:N}$ remains relatively constant from low to high T_{eff} ranges, in agreement with the co-variation of POC and PON fluxes at the upper and lower traps and of T_{eff} and T_{effPON} (Fig. S2b & d). During the remineralisation-like configuration, the vertical C:P and N:P transfer efficiencies sharply decrease by a factor of 3 from intermediate to low $T_{effC:P}$ and $T_{effN:P}$ reaching ~35% (Tab. 3b). These $T_{effC:P}$ and $T_{effN:P}$ decreases are in line with a potential relative enrichment of more refractory phosphorous materials. Also, C:P and N:P ratios are higher in the upper trap and become lower in the lower trap than the classical values. Analysis of the transfer efficiency of the molar ratios involving BSi is more complex. $T_{effSi:C}$ and $T_{effSi:N}$ remain relatively constant for the three T_{eff} ranges. However, $T_{effSi:P}$ presents a huge decrease by a factor of 7 from high to low T_{eff} ranges. The antagonist interplay of the refractory BSi properties and the dissolution effect on BSi (e.g. Loucaides et al., 2008) must be considered, in addition to recycling mainly occurring at the sediment/water interface (e.g. Tréguer and De La Rocha, 2013).

The $CaCO_3$ flux collected in the deep trap appears to be about twice as high as the global average in preservation-like configurations (high T_{eff}; Tab. 3c&S5). The high T_{eff} range is characterized by $T_{effCaCO3}$ higher than 100% (133%). A potential accumulation and/or aggregation of calcium carbonate particles, known for their refractory properties, (e.g. from coccolithophorids or planktonic foraminifera) with depth could be responsible. The comparison from high to intermediate T_{eff} ranges shows a $T_{effCaCO3}$ decrease of twice the amount as for the other components (T_{eff}, T_{effPON}, T_{effPOP} and T_{effBSi}). The $T_{effCaCO3}$ decrease could simply be related to changes in the composition of the calcifying plankton community in the surface layer, or possibly in the subsurface OMZ. However, the relative constancy, especially in the upper trap, regarding the elemental composition in the reported fluxes, the swimmer communities and the upper $CaCO_3$ flux (cf Fig. 6b, Tab. 2 and 3), suggests that the $T_{effCaCO3}$ decrease could be associated with a stimulation of significant water column dissolution. Since the intermediate T_{eff} range corresponds to a large predominance of ~90 $AMOP_{summer}$ samples (~90%, Tab. 1), the explanation is focused on $AMOP_{summer}$ only and based on the following consideration:

The $CaCO_3$ transfer efficiency could be modulated partly by pH conditions, and partly as a consequence of ballast. Indeed, OMZs are characterized by low pH conditions (Paulmier and Ruiz-Pino, 2009; Paulmier et al., 2011; Leon et al., 2011) and may induce calcite dissolution (e.g. Orr et al., 2005). As low pH was recorded in a cross-shore section during the AMOP cruise (austral summer 2014, Fig. S3), $CaCO_3$ dissolution could potentially be considered as a factor acting on $CaCO_3$ transfer in $AMOP_{summer}$ samples. Moreover, because of the refractory nature of $CaCO_3$, it could accumulate along the water column. This potential $CaCO_3$ accumulation could explain the high transfer efficiency. Ballasting could therefore explain the transfer efficiency of over 100 % for some samples. Note however that the error bar on $T_{effCaCO3}$ is high, and thus does not allow precise differentiation between these invoked processes.

In line with paleoceanographic studies, it should be interesting to focus on the evolution of particulate $\delta^{13}C$ and $\delta^{15}N$ as a function of the T_{eff} ranges. T_{eff13C} and T_{eff15N} remain around 100% whatever the T_{eff} ranges (Fig. 7, Tab. 3c). While $\delta^{13}C$ appears to slightly decrease during particle sinking (average T_{eff13C} of 95%; Tab. S4), no significant T_{eff13C} distinction between low, intermediate and high T_{eff} ranges could be made. For all T_{eff} ranges and all considered seasons, carbon isotope is slightly heavier in the lower trap (Tab. S4). The enrichment in heavy isotopes with depth potentially indicates an increasing influence of inorganic carbon with depth. The T_{eff15N} variation appears to be stronger than T_{eff13C}, varying between 83 and 267% (average of 125% ± 37%). T_{eff15N} remains high (~100% and higher) with variations up to 40%. The highest T_{eff15N} (156%) occurs for the intermediate T_{eff} range. But T_{eff15N} is lower for low and high T_{eff} ranges (107 and 113%, respectively). The T_{eff15N} differences between ranges could be linked to the vertical alteration of particulate $\delta^{15}N$ distribution associated with the OMZ oxycline and core structure (Libes and Deuser, 1988). The three T_{eff} range configurations could correspond to different: i) chemical and isotopic PON compositions associated with different metabolic pathways of OM synthesis; ii) oxycline depths and/or oxygenations impacting the microbial activities and the OM degradation processes. The alteration to particulate $\delta^{15}N$ is potentially due to the microbial activities and chemical and isotopic PON compositions associated with the different metabolic pathways of OM synthesis. In addition, the depth and oxygenation of the oxycline should play an important role in explaining the differences between low, intermediate and high T_{eff} ranges. However, one should be cautious with these results, as the variability in $\delta^{15}N$ on the entire dataset does not allow strict differentiation between the ranges.

Therefore, in the OMZ, short-term $[O_2]$ fluctuations and particle loading appear to be significant. They should be considered for further studies on OM fate, carbon sequestration, nutrient regeneration, and the production or consumption of greenhouse and toxic dissolved gas. These effects call for the development of variable molar ratio models for OM production mechanisms, and OMZ remineralisation processes, and for the revised interpretation of paleoproxies.

Summary and conclusion

The seasonal and intraseasonal analysis of particles collected using sediment traps in the oxycline and the core of the Peruvian EBUS, confirms that the OMZ can behave either as a recycling or a preservation system for Organic Matter (OM). Transfer efficiency (T_{eff}) presents variations which can be classified into three main characteristic ranges: high with $50<T_{eff}<75\%$ associated with preservation capacity; intermediate with $20<T_{eff}<50\%$; low with $T_{eff}<6\%$, associated with remineralization capacity. These T_{eff} variations represent a more or less efficient carbon export through the OMZ. Seasonally, two different steady states are defined for oxygen conditions. The suboxic regime ($[O_2]<25$ µmol.kg^{-1}) occurs mainly in austral summer. The hypoxic/oxic regime occurs in austral winter and early spring ($15<[O_2]<160$ µmol.kg^{-1}). Suboxia is expected to foster OM preservation and therefore enhance transfer efficiency. But low O_2 conditions occurring in austral summer can also induce weak remineralisation, consequently to intraseasonal wind-driven oxygenation events. In addition to oxygenation conditions, sinking particles from the oxycline play a role in transfer efficiency. Indeed, the high POC flux (> 80 mgC.m^{-2}.d^{-1}) end of winter/early spring can provide enough substrates to sustain the anabolic requirement of the microbial activity, and shut down the vertical transfer ($T_{eff}<6\%$). In contrast, the extreme deficits in oxygen ($[O_2]<$ 5 µmol.kg^{-1} at the oxycline) or OM (<40 mgC.m^{-2}.d^{-1}) are considered as a limitation for OM degradation activity (e.g. microbial remineralisation and zooplankton feeding on particles). These configurations correspond to the most efficient POC transfer ($T_{eff}>50\%$) for both summer and winter seasons. Between high and low T_{eff}, higher levels of O_2 or OM, even in a co-limitation context, can lead to slightly decreased OMZ transfer efficiency ($20<50\%$), especially in summer ($20<40\%$). For all sampling seasons, particle composition could be considered as stable, mainly composed of POC and BSi. The stable particle composition thus does not allow a full investigation of the question of the impact of OM quality. In the time and spatial location covered by this study, OM quality does not seem to be the main factor leading to T_{eff} modulation. Only punctually, the occurrence of nitrogen-rich organic compounds in relatively well oxygenated water could strengthen remineralisation activity, with low intermediate T_{eff} (32%). This study reconciles two opposite views concerning the effects of OMZ behaviour on OM cycling. It supports the existence of both dynamic and static balanced biogeochemical states defined as states with and without significant remineralisation and O_2 consumption, respectively. The key microbial feedback on particles including their elemental composition should be further investigated as well as detailing the role of OM quality. This is expected to lead to a better understanding of the vertical OM transfer efficiency of the OMZ and its modulation. Climate projections and paleoceanography studies should therefore consider the intermittence of the OMZ preservation or recycling capacity, crucial for global biogeochemical budgets.

Acknowledgements

We would like to thank the crew of the German R/V Meteor for the deployment as part of the DFG-funded SFB754 fieldwork, the crew of the Peruvian R/V Olaya for the visit and the crew of the French R/V Atalante for the recovery of the fixed AMOP mooring. We would like to thank Stefan Sommer and Marcus Dengler for providing the METEOR wind dataset. We would also like to thank Miriam Soto, Anne Royer and Emmanuel De Saint Léger for general logistics and administrative support. We are grateful to Vincent Rossi for discussions regarding the processes affecting the sinking speed of the particles. We are grateful to both anonymous reviewers for their comments which greatly improved our manuscript. We are finally also grateful to Christophe Lerebourg, from ACRI-ST for his support during the course of this study. This work was supported by the AMOP ("Activity of

research dedicated to the Minimum of Oxygen in the eastern Pacific") project supported by IRD, CNRS/INSU, DT-INSU and LEGOS, and by a GIS COOC (UPMC, INSU/CNRS, CNES, ACRI-ST) Ph.D. grant.

Literature cited

Azam, F., Steward, G. F., Smith, D. C. and Ducklow, H. W.: Significance of bacteria in carbon fluxes in the Arabian Sea, Earth Planet. Sci., 103(2), 341-351, 1994.

Baker, E. T., Milburn, H. B. and Tennant, D. A.: Field assessment of sediment trap efficiency under varying flow conditions, J. Mar. Res., 46(3), 573-592, 1988.

Bardhan, P., Karapurkar, S. G., Shenoy, D. M., Kurian, S., Sarkar, A., Maya M. V., Naik, H., Varik, S. and Naqvi, S. W. A.: Carbon and nitrogen isotopic composition of suspended particulate organic matter in Zuari Estuary, west coast of India, J. Mar. Syst., 141, 90-97, 2015.

Berelson W. M.: The flux of particulate organic carbon into the ocean interior: A comparison of four U.S. JGOFS regional studies, Oceanography., 14(4), 59-67, 2001.

Böning, P., Brumsack, H. J., Böttcher, M. E., Schnetger, B., Kriete, C., Kallmeyer, J. and Borchers, S. L.: Geochemistry of Peruvian near-surface sediments, Geochimica and Cosmochimica Acta., 68(21), 4429-4451 2004.

Brzezinski, M. A.: The Si: C: N ratio of marine diatoms: interspecific variability and the effect of some environmental variables, Journal of Phycology, 21(3), 347-357, 1985.

Buesseler, K. O., Lamborg, C. H., Boyd P. W., Lam, P. J., Trull, T. W., Bidigare, R. R., Bishop, J. K. B., Casciotti, K. L., Dehairs, F., Elskens, M., Honda, M., Karl, D. M., Siegel, D. A., Silver, M. W., Steinberg, D. K., Valdes, J., Van Mooy, B. and Wilson S.: Revisiting carbon flux through the ocean's twilight zone, Science, 316, 567–570, 2007.

Cabré, A., Marinov, I., Bernardello, R., and Bianchi, D. Oxygen minimum zones in the tropical Pacific across CMIP5 models: mean state differences and climate change trends. Biogeosciences, 12(18), 5429-5454, 2015.

Chaigneau, A., Domingez, N., Eldin, G., Flores, R., Grados, C. and Echevin, V.: Near-Coastal circulation in the Northern Humboldt Current System from shipboard ADCP data, J. Geophys. Res., 118(10), 5251-5266, 2013.

Chavez, F. P. and Messié, M.: A comparison of Eastern Boundary Upwelling Ecosystems, Prog. Oceanogr., 83, 80-96, 2009.

Chavez, F. P., Bertrand, A., Guevara-Carraso, R. and Csirke, J.; The northern Humboldt Current System: Brief history, present status and a view towards the future, Prog Oceanogr., 79, 95-105, 2008.

Chi Fru, E., Rodriguez, N.P., Partin, C. A., Lalonde, S. V., Andersson, P., Weis, D. J., El Albani A., Rodushkin, I. and Konhauser, K. O.: Cu isotopes in marine black shales record the Great Oxidation Event, Proc Natl Acad Sci USA., 113(18), 4941-4946, 2016.

de Boyer Montegut, C., Fischer, A. S., Lazar, A. and Iudicone, D.: Mixed layer depth over the global ocean: An examination of profile data and a profile-based climatology, J. Geophys. Res., 109, C12003, 2004.

Degens, E. T., Behrendt, M., Gotthard, B. and Reppmann, E.: Metabolic fractionation of carbon isotopes in marine plankton-II, Data on samples collected off the coasts of Peru and Ecuador. Deep Sea Res. 15, 11-20, 1968.

DeMaster, D. J.: The supply and accumulation of silica in the marine environment, Geochimica acta, 45(10), 1715-1732, 1981.

Devol, A. H.: Bacterial oxygen uptake kinetics as related to biological processes in oxygen deficient zones of the oceans, Deep Sea Res. 25, 137-146, 1978.

Devol, A. H., and Hartnett, H. E. Role of the oxygen-deficient zone in transfer of organic carbon to the deep ocean, Limnology and Oceanography, 46(7), 1684-1690, 2001.

Dewitte, B., Illig, S., Renault, L., Gourbanova, K., Takahashi, K. and Gushchina, D.: Modes of variability between sea surface temperature and wind stress intraseasonal anomalies along the coast of Peru from satellite observation, J. Geophys. Res. 116, 04028, doi:10.1029/2010JC006495, 2011.

Dewitte, B., Vazquez-Cuervo, J., Goubanova, K., Illig, S., Takahashi, K., Cambon, G., Purca, S., Correa, D., Gutierrez, D., Sifeddine, A. and Ortlieb, L.: Change in El Niño flavours over 1958-2008: Implications for the long-term trend of the upwelling off Peru, Deep Sea Res II, 77-80, 143-156, 2012.

Diaz, J., Ingall, E., Benitez-Nelson, C., Paterson, D., de Jonge, M. D., McNulty, I. and Brandes, J. A.: Marine polyphosphate: a key player in geologic phosphorus sequestration, Sciences, 320, 652-655, 2008.

Garcia-Robledo, E., Padilla, C. C., Aldunate, M., Stewart, F. J., Ulloa, O., Paulmier, A., Gregori, G. and Revsbech, N. P.: Cryptic Oxygen cycling in Anoxic Marine Zones, Proc. Natl. Acad. Sci. U.S.A., 114(31), 8319-8324, doi:10.1073/pnas.1619844114, 2017.

Heimburger, L. E., Lavigne, E., Migon, C., D'ortenzio, F., Estournel, C., Coppola, L. and Miquel, J. C. Temporal variability of vertical flux at the DYFAMED time-series station (Northwestern Mediterranean Sea), Prog. Oceanogr., 119, 59-67, 2013.

Helmke, P., Romero, O. and Fischer, G.: Northwest African upwelling and its effect on offshore organic carbon export to the deep sea, Global Biogeochem. Cycles, 19, GB4015, 2005.

Hirata, T., Hardman-Mountford, N. J., Brewin, R. J. W., Aiken, J., Barlow, R., Suzuki, K., Isada, T., Howell, T., Hashioka, T., Noguchi-Aita, M. and Yamanaka, Y.: Synoptic relationships between surface Chlorophyll-a and diagnostic pigments specific to phytoplankton functional types, Biogeosciences, 8(2), 311-327, 2011.

Illig, S., Dewitte, B., Goubanova K., Cambon, G., Boucharel, J., Monetti, F., Romero, C., Purca, S. and Flores, R.: Forcing mechanisms of intraseasonal SST variability off central Peru in 2000–2008, J. Geophys. Res. Oceans, 119, 3548–3573, doi:10.1002/2013JC009779, 2014.

Kalvelage, T., Lavik, G., Lam, P., Contreras, S., Arteaga, L., Löscher, C. R. and Kuypers, M. M.: Nitrogen cycling driven by organic matter export in the South Pacific oxygen minimum zone, Nature geoscience, 6(3), 228-234, 2013.

Keil, R. G., Neibauer, J. A., Biladeau, C., van der Elst, K. and Devol, A. H.: A multiproxy approach to understanding the « enhanced » flux of organic matter through the oxygen-deficient waters of the Arabian Sea, Biogeosciences. 13, 2077-2092, 2016.

Lam, P., Lavik, G., Jensen, M. M., Van de Vossenberg, J., Schmidt, M., Woebken, D., Gutierez, D., Amann, M., Jetten, S. M. and Kuypers, M. M.: Revising the nitrogen cycle in the Peruvian oxygen minimum zone, Proc. Natl. Acad. Sci. U.S.A., 106(12), 4752-4757, 2009.

Lampitt, R. S., Noji, T. and Von Bodungen, B.: What happens to zooplankton faecal pellets? Implications for material flux, Marine Biology, 104.1, 15-23, 1990.

Law, C. S., Brévière, E., De Leeuw, G., Garçon, V., Guieu, C., Kieber, D. J., Kontradowitz, S., Paulmier, A., Quinn, P. K., Saltzman, E. S., Stefels, J. and von Glasow, R.: Evolving research directions in surface ocean–lower atmosphere (SOLAS) science, Environ Chem., 10.1071/EN12159, 2012.

León, V., Paulmier, A., Ledesma, J., Croot, P., Graco, M., Flores, G., Morón, O. and Tenorio, J.: pH como un Trazador de la Variabilidad Biogeoquímica en el Sistema de Humboldt, Boletin del IMARPE, 26(1-2), 2011.

Lewis, E. and Wallace, D. W. R.: Program Developed for CO2 System Calculations, Edited by ORNL/CDIAC-105a., Carbon Dioxide Information Analysis Center, Oak Ridge National Laboratory, U.S. Department of Energy, Oak Ridge, Tennessee, 1998.

Libes, S. M. and Deuser, W. G.: The isotope geochemistry of particulate nitrogen in the Peru upwelling area and the Gulf of Maine, Deep Sea Research Part A, Oceanographic Research Papers, 35(4), 517-533, 1988.

Lipschultz, F., Wofsy, S.C., Ward, B. B., Codispoti, L. A., Friedrich, G., Elkins, J. W.: Bacterial transformations of inorganic nitrogen in the oxygen deficient waters of the Eastern Tropical South Pacific Ocean, Deep Sea Res., 35(10), 1513-1541, 1990.

Loucaides, S., Van Capellen, P. and Behrends, T: Dissolution of biogenic silica from land to ocean: Role of salinity and pH, Limnol Oceanogr., 53(4), 1614-1621, 2008.

Lueker, T. J., Dickson, A. G. and Keeling, C. D.: Ocean pCO2 calculated from dissolved inorganic carbon, alkalinity, and equations for K1 and K2: validation based on laboratory measurements of CO2 in gas and seawater at equilibrium, Marine Chemistry, 70(1–3), 105-119, 2000.

Martin J. H., Knauer, G. A., Karl, D. M. and Broenkow, W. W.: VERTEX: carbon cycling in the NE Pacific, Deep Sea Res., 34, 267-285, 1987.

Marsay, C. M., Sanders, R. J., Henson, S. A., Pabortsava, K., Achterberg, E. P. and Lampitt, R. S.: Attenuation of sinking particulate organic carbon flux through the mesopelagic ocean, Proc. Natl. Acad. Sci. U.S.A., 112(4), 1089-1094, 2015.

Mayers, P. A.: Preservation of elemental and isotopic source identification of sedimentary organic matter, Chem. Geol., 114, 239-302, 1993.

McDonnell, A. M. P., Boyd, P. W. and Buesseler, K. O.: Effects of sinking velocities and microbial respiration rates on the attenuation of particulate carbon fluxes through the mesopelagic zone, Global Biogeochem. Cycles, 29(2), 175-193, 2015.

Miquel, J. C., Martin, J., Gasser, B., Rodrigez-y-Baena, A., Toubal, T. and Fowler, S. W.: Dynamics of particles flux and carbon export in the northwestern Mediterranean Sea: A two scale time-series study at the DYFAMED site, Prog. Oceanogr., 91, 451-481, 2011.

Moffitt, S. E., Moffitt, R. A., Sauthoff, W., Davis, C. V., Hewett, K. and Hill, T. M.: Paleoceanographic Insights on Recent Oxygen Minimum Zone Expansion: Lessons for Modern Oceanography, PLoS ONE, 10(1): e0115246, 2015.

Montes, I., Colas, F., Capet, X. and Schneider, W.: On the pathways of the equatorial subsurface currents in the eastern equatorial Pacific and their contribution to Peru-Chile Undercurrent, J. Geophys. Res., 115, C09003, doi:10.1029/2009JC005710, 2010.

Oschlies, A., Duteil, O., Getzlaff, J., Koeve, W., Landolfi, A., and Schmidtko, S. Patterns of deoxygenation: sensitivity to natural and anthropogenic drivers, Phil. Trans. R. Soc. A, 375(2102), 20160325, 2017.

Ohkouchi, N., Ogawa, N. O., Chikaraishi, Y., Tanaka, H. and Wada, E.: Biochemical and physiology bases for the use of carbon and nitrogen isotopes in environmental and ecological studies, Prog. Earth Planet. Sci., 2:1, doi: 10.1186/s40645-015-0032-y, 2015.

Orr, J. C. et al.: Anthropogenic ocean acidification over the twenty-first century and its impact on calcifying organisms, Nature, 437, 681-686, doi:10.1038/nature04095, 2005.

Packard, T. T., Osma, N., Fernández-Urruzola, I., Codispoti, L. A., Christensen, J. P. and Gómez, M.: Peruvian upwelling plankton respiration: calculations of carbon flux, nutrient retention efficiency, and heterotrophic energy production, Biogeosciences, 12, 2641-2654, doi:10.5194/bg-12-2641-2015, 2015.

Pantoja, S., Sepulveda, J. and Gonzalez, H. E.: Decomposition of sinking proteinaceous material during fall in the oxygen minimum zone off northern Chile, Deep Sea Res. I., 51, 55-70, 2004.

Paulmier, A., Ruiz-Pino, D., Garçon, V. and Farias, L.: Maintaining of the Eastern South Pacific Oxygen Minimum Zone (OMZ) off Chile, Geophys. Res. Lett., 33(20), L20601, 2006.

Paulmier, A., Ruiz-Pino, D. and Garçon, V.: The oxygen minimum zones (OMZ) off Chile as intense source of CO_2 and N_2O, Cont. Shelf Res., 28(20), 2746-2756, 2008.

Paulmier, A., Kriest, I. and Oschlies, A.: Stoichiometries of remineralisation and denitrification in global biogeochemical ocean models, Biogeosciences, 6, 923–935, doi:10.5194/bg-6-923-2009, 2009.

Paulmier, A. and Ruiz-Pino, D.: Oxygen minimum zones (OMZs) in the modern ocean, Prog. Oceanogr., 80(3-4), 113-128, 2009.

Pennington, J. T., Mahoney, K. L., Kuwahara, V. S., Kolber, D. D., Calnies, R. and Chavez, F. P.: Primary production in the eastern tropical Pacific: A review, Prog. Oceanogr., 66, 285-317, 2006.

Ramaiah, N., Raghukumar, S. and Gauns, M.: Bacterial abundance and production in the central and eastern Arabian Sea, Current Science, 71(11), 878-882, 1996.

Redfield, A. C., Ketchum, B. H. and Richards, F. A., The influence of organism on the composition of the seawater, The Sea, 2, edited by M. N. Hill, pp 26-77, Interscience, New-York, 1963.

Roullier, F., Berline, L., Guidi, L., Durrieu De Madron, X., Picheral, M., Sciandra, A., Pesant, S., and Stemmann, L.: Particle size distribution and estimated carbon flux across the Arabian Sea oxygen minimum zone, Biogeosciences, 11, 4541-4557, https://doi.org/10.5194/bg-11-4541-2014, 2014.

Siegel, D. A., Granata, T. C., Michaelis, A. F. and Dickey, T. D.: Mesoscale eddy diffusion, particle sinking and the interpretation of sediment trap data, J. Geophys. Res., 95(C4), 5305-5311, 1990.

Sobarzo, M., Bravo, L., Donoso, D., Garcès-Vargas, J. and Schneider, W.: Coastal upwelling and seasonal cycles that influence the water column over the continental shelf of central Chile, Prog. Oceanogr., 75, 363-382, 2007.

Stemmann, L., Jackson, G. A. and Ianson, D.: A vertical model of particle size distributions and fluxes in the midwater column that includes biological and physical processes-Part I: model formulation, Deep Sea Res. Part. I., 51, 865-884, 2004.

Stemmann, L. and Boss, E.: Plankton and particle size and packaging: from determining optical properties to driving the biological pump, Annu. Rev. Mar. Sci., 4, 263–290, 2012.

Stewart, F. J., Ulloa, O. and DeLong, E. F.: Microbial metatranscriptomics in a permanent marine oxygen minimum zone, Environ. Microbiol., 14(1), 23-40, 2012.

Strickland, J. D. H. and Parsons, T. R.: A practical handbook of sea water analysis, The fisheries research board of Canada, Bulletin N°25, 1972.

Suess, E.: Particulate organic carbon flux in the ocean-surface productivity and oxygen utilization, Nature, 288, 206-263, 1980.

Sun, M-Y., Aller, R. C., Lee C. and Wakeham, G.: Effect of oxygen and redox oscillation on degradation of cell-associated lipids in superficial marine sediments, Geochemica and Cosmochimica Acta, 66(11), 2003-2012, 2002.

Taylor G. T., Thunell R. C., Varela R., Benitez-Nelson C. R., Astor Y.: Hydrolytic ectoenzyme activity associated with suspended and sinking organic particles within the anoxic Cariaco Basin, Deep Sea Research I, 56, 2009.

Thunell, R. C., Varela, R., Llano, M., Collister, J., Karger, F. M., and Bohrer, R.: Organic carbon fluxes, degradation, and accumulation in an anoxic basin: sediment trap results from the Cariaco Basin, Limnology and Oceanography, 45(2), 300-308, 2000.

Van Mooy, B. A. S., Keil, R. G. and Devol, A. H.: Impact of suboxia on sinking particulate organic carbon: enhanced carbon flux and preferential degradation of amino-acids via denitrification, Geochimica and Cosmochimica Acta, 66(3), 457-465, 2002.

Waniek, J., Koeve, W., Prien, D.: Trajectories of sinking particles and the catchment areas above sediment traps in the northeast Atlantic, J. Mar. Res., 58, 983-1006, 2000.

Tables captions

Table 1: ***POC flux, transfer efficiency T_{eff} and b for each main T_{eff} range***. *T_{eff} is determined from $\%Flux_{149m}/Flux_{34m}$ (Eq. 1). b is the coefficient from the Martin's curves theory (Suess, 1980; Martin et al., 1987). Italic and non-italic values correspond to the fluxes at 34 m and 149 m, respectively. On the last lines of the table, bold colored values in red, yellow and blue correspond to POC fluxes, T_{eff} and b averaged values for low, intermediate and high T_{eff} ranges, respectively, with the relative standard deviation between samples (±SD%). Analysis accuracy on the POC fluxes is ±0.2%, inducing an absolute uncertainty on its vertical transfer efficiency estimated from a logarithmic expansion of ±0.2% (cf. Methods).*

Table 2: ***Oxygen concentration in the upper and bottom OMZ layer, proportion of Polychaetes number of individuals, and POC flux/O_2 concentration ratios***. *O_2 concentration corresponds to the oxygen concentration averaged on the sampling acquisition periods: $\overline{[O_2]}_{7days_15min}$ for $AMOP_{summer}$ (denoted AMOP1) and $\overline{[O_2]}_{11days_15min}$ for $AMOP_{winter\text{-}spring}$ (denoted AMOP2). %Poly corresponds to the percentage of number of individuals of Polychaetes relatively to all collected swimmers, per day. The POC flux / O_2 concentration corresponds to the ratio of both weekly quantities (POC flux collected in the trap and $\overline{[O_2]}_{1week_15min}$ determined from the O_2 sensor). Italic values correspond to the [O_2], %Poly and POC flux / O_2 concentration at the upper trap, and non-italic values at the lower trap. On the last lines of the table, bold colored values in red, yellow and blue correspond to[O_2], %Poly and POC flux /[O_2] averaged values for low, intermediate and high T_{eff} ranges, respectively, with the relative standard deviation between samples (±SD%). %Poly is determined from a significant number of Polychaetes individuals collected per sample (4607 in average, between 50 and 31099). Note that Polychaetes and copepods represent 97% of all the reported swimmers.*

Table 3: ***Organic elemental fluxes and the corresponding molar ratios as well as inorganic and isotopic fluxes, and their transfer efficiencies for each main T_{eff} range.***

a) Organic Elementary fluxes in mg.m^{-2}.d^{-1} and their transfer efficiency in % (T_{eff}, T_{effPON}, T_{effPOP}, T_{effBSi}; cf. Table 1 caption for calculation) in terms of Particulate Organic Carbon (POC), Nitrogen (PON), Phosphorus (POP) and biogenic Silica (BSi) for each three main T_{eff} ranges (low in red, intermediate in yellow, high in blue) with the temporal standard deviation between samples (±SD%). Italic and non-italic values correspond to the fluxes at 34 m and 149 m, respectively. Analysis accuracies on the elementary fluxes are ±0.2% for both POC and PON, ±3% for POP, and ±5% for BSi, inducing an absolute uncertainty of ±0.2% (T_{eff}), ±0.2% (T_{effPON}), ±3% (T_{effPOP}) and ±5% (T_{effBSi}) on the transfer efficiency (cf. Methods).

b) Values of elementary ratios (C:N, C:P, N:P, and Si:C, Si:N, Si:P) and transfer efficiency of these ratios in % ($T_{effC:N}$, $T_{effC:P}$, $T_{effN:P}$, and $T_{effSi:N}$, $T_{effSi:N}$, $T_{effSi:P}$; cf. Table 1 caption for calculation) for each three main T_{eff} ranges (low in red, intermediate in yellow, high in blue) with the temporal standard deviation between samples (±SD%). Italic and non-italic values correspond to the fluxes at 34 m and 149 m, respectively. Analysis accuracies on the elementary ratios are ± 0.4, 3.2, 3.2% and ± 5.2, 5.2, 8% for C:N, C:P and N:P and for Si:C, Si/N and Si:P, respectively, inducing an absolute uncertainty of ±0.9% ($T_{effC:N}$), ±6.3% ($T_{effC:P}$), ±6% ($T_{effN:P}$), and of ±12% ($T_{effSi:C}$), ±13.4% ($T_{effSi:N}$) and ±19% ($T_{effSi:P}$) on the transfer efficiency (cf. Methods). Classical (reference) molar ratios have been reported on the second lines from Redfield et al. (1963) and Brezinski (1985).

c) Fluxes of inorganic calcium carbonate ($CaCO_3$) in mgCa.m^{-2}.d^{-1} and of carbon isotopic ratio ($\delta^{13}C$) and nitrogen isotopic ratio ($\delta^{15}N$) in ‰ and their transfer efficiency in % ($T_{effCaCO3}$, T_{eff13C}, T_{eff15N}; cf. Table 1 caption for calculation) for each three main T_{eff} ranges (low in red, intermediate in yellow, high in blue) with the temporal standard deviation between samples (±SD%). Italic and non-italic values correspond to the fluxes at 34 m and 149 m, respectively. Analysis accuracies on the elementary fluxes are ±3% for $CaCO_3$, ±0.006‰ for $\delta^{13}C$ and ±0.007‰ for $\delta^{15}N$, inducing an absolute uncertainty of ±3% ($T_{effCaCO3}$), ±0.06% (T_{eff13C}) and ±0.26% (T_{eff15N}) on the transfer efficiency (cf. Methods).

Sample name	Date in 2013 Start	End	POC Fluxes mgC.m^{-2}.d^{-1} *34 m*	149 m	Teff %	Error bar on Teff %	b
AMOP-S1	**06/01**	**13/01**	*139.40*	98.63	71	± 1	0.23
AMOP1-S2	**13/01**	**20/01**	*127.87*	70.68	55	± 1	0.40
AMOP1-S3	**20/01**	**27/01**	*149.48*	85.89	57	± 1	0.37
AMOP1-S4	**27/01**	**03/02**	*92.16*	22.14	24	± 1	0.97
AMOP1-S5	**03/02**	**10/02**	*107.43*	45.49	42	± 1	0.58
AMOP1-S6	**10/02**	**17/02**	*132.72*	41.49	31	± 1	0.79
AMOP1-S7	**17/02**	**24/02**	*41.16*	17.98	44	± 2	0.56
AMOP1-S8	**24/02**	**03/03**	*86.33*	20.44	24	± 1	0.98
AMOP1-S9	**03/03**	**10/03**	*109.69*	37.92	35	± 1	0.72
AMOP1-S10	**10/03**	**17/03**	*51.31*	19.25	38	± 3	0.66
AMOP1-S11	**17/03**	**24/03**	*20.30*	11.63	57	± 8	0.38
AMOP1-S12	**24/03**	**31/03**	*54.08*	20.14	37	± 2	0.67
AMOP2-S1	**28/06**	**09/07**	*41.19*	55.49	135	± 2	-0.20
AMOP2-S2	**09/07**	**20/07**	*37.05*	21.15	57	± 1	0.38
AMOP2-S3	**20/07**	**31/07**	*17.15*	18.18	106	± 5	-0.04
AMOP2-S4	**31/07**	**11/08**	*19.42*	6.21	32	± 4	0.77
AMOP2-S5	**11/08**	**22/08**	*17.91*	12.22	68	± 4	0.26
AMOP2-S6	**22/08**	**02/09**	*6.45*	9.59	149	± 12	-0.27
AMOP2-S7	**02/09**	**13/09**	*470.49*	8.28	2	± 0.1	2.73
AMOP2-S8	**13/09**	**24/09**	*395.10*	4.93	1	± 0.1	2.97
AMOP2-S9	**24/09**	**05/10**	*172.94*	7.20	4	± 0.3	2.15
AMOP2-S10	**05/10**	**16/10**	*135.00*	6.97	5	± 0.3	2.01
AMOP2-S11	**16/10**	**27/10**	*180.91*	4.78	3	± 0.2	2.46
AMOP2-S12	**27/10**	**07/11**	*83.04*	3.00	4	± 1	2.25
	High Teff		***71*** (±89%)	**40** (±88%)	**59** (±9%)		**0.36** (±16%)
	Intermediate Teff		***77*** (±49%)	**26** (±50%)	**34** (±21%)		**0.74** (±20%)
	Low Teff		***240*** (±65%)	**6** (±33%)	**3** (±48%)		**2.43** (±15%)

Table 1

Sample name	Date in 2013 Start	End	$[O_2]$ µmol.kg^{-1} *34 m*	147 m	%Poly %/day *34 m*	POC/$[O_2]$ *34 m*
AMOP-S1	**06/01**	**13/01**	*6.74*	3.09	*12.4*	*20.7*
AMOP-S2	**13/01**	**20/01**	*3.48*	3.08	*13.2*	*36.7*
AMOP1-S3	**20/01**	**27/01**	*4.91*	3.07	*11.7*	*30.4*
AMOP1-S4	**27/01**	**03/02**	*6.23*	3.06	*9.7*	*14.8*
AMOP1-S5	**03/02**	**10/02**	*4.5*	3.07	*13.6*	*23.9*
AMOP1-S6	**10/02**	**17/02**	*5.49*	3.07	*8.9*	*24.2*
AMOP1-S7	**17/02**	**24/02**	*3.73*	3.06	*3.8*	*11.0*
AMOP1-S8	**24/02**	**03/03**	*12.52*	3.07	*6.3*	*6.9*
AMOP1-S9	**03/03**	**10/03**	*9.37*	3.07	*1.0*	*11.7*
AMOP1-S10	**10/03**	**17/03**	*6.03*	3.02	*11.4*	*8.5*
AMOP1-S11	**17/03**	**24/03**	*4.33*	3.01	*14.1*	*4.7*
AMOP1-S12	**24/03**	**31/03**	*3.86*	3.02	*13.8*	*14.0*
AMOP2-S1	**28/06**	**09/07**	*34.1*	3.62	0.7	*1.21*
AMOP2-S2	**09/07**	**20/07**	*41.35*	3.56	1.1	*0.9*
AMOP2-S3	**20/07**	**31/07**	*56.69*	4.05	0.8	*0.3*
AMOP2-S4	**31/07**	**11/08**	*66.22*	4.85	0.1	*0.3*
AMOP2-S5	**11/08**	**22/08**	*115.7*	11.84	0.0	*0.2*
AMOP2-S6	**22/08**	**02/09**	*69.35*	5.76	0.1	*0.1*
AMOP2-S7	**02/09**	**13/09**	*89.06*	6.33	0.3	*5.3*
AMOP2-S8	**13/09**	**24/09**	*31.61*	4.65	0.4	*12.5*
AMOP2-S9	**24/09**	**05/10**	*38.2*	4.85	0.6	*4.5*
AMOP2-S10	**05/10**	**16/10**	*68.63*	4.43	0.3	*2.0*
AMOP2-S11	**16/10**	**27/10**	*100.15*	3.59	0.4	*1.8*
AMOP2-S12	**27/10**	**07/11**	*34.22*	3.08	0.6	*2.4*
	High Teff		***34.0*** **(±143%)**	**4.9** **(±79%)**	***8.0*** **(±86%)**	***14.6*** **(±121%)**
	Intermediate Teff		***13.1*** ***(±154%)***	**3.2** ***(±18%)***	***7.6*** ***(±67%)***	***12.8*** ***(±60%)***
	Low Teff		***60.3*** **(±50%)**	**4.5** **(±25%)**	***0.4*** **(±35%)**	***4.7*** **(±85%)**

Table 2

a)	PON mgN.m^{-2}.d^{-1}		T_{effPON} %	POP mgP.m^{-2}.d^{-1}		T_{effPOP} %	BSi mgSi.m^{-2}.d^{-1}		T_{effBSi} %
	34 m	149 m		*34 m*	149 m		*34 m*	149 m	
High Teff	***10.56***	**5.66**	**54**	***3.29***	**1.41**	**60**	***75.36***	**53.34**	**72**
	(±85%)	**(±87%)**	**(±89%)**	***(±91%)***	**(±63%)**	**(±53%)**	***(±78%)***	**(±72%)**	**(±32%)**
Intermediate Teff	***10.72***	**3.66**	**34**	***3.71***	**1.21**	**34**	***69.03***	**26.15**	**37**
	(±46%)	**(±56%)**	**(±27%)**	***(±33%)***	**(±50%)**	**(±47%)**	***(±54%)***	**(±58%)**	**(±25%)**
Low Teff	***41.23***	**0.91**	**2**	***4.93***	**0.53**	**14**	***495.00***	**9.47**	**3**
	(±61%)	**(±18%)**	**(±47%)**	**(±64%)**	**(±98%)**	**(±81%)**	**(±105%)**	**(±81%)**	**(±119%)**

b)	C:N 6.63		$T_{effC:N}$ %	C:P 106		TeffC:P %	N:P 16		$T_{effN:P}$ %
	34 m	149 m		*34 m*	149 m		*34 m*	149 m	
High Teff	***7.59***	**8.26**	**111**	***60.72***	**68.01**	**117**	***8.3***	**8.26**	**112**
	(±13%)	**(±6%)**	**(±16%)**	***(±31%)***	**(±39%)**	**(±41%)**	***(±44%)***	**(±37%)**	**(±49%)**
Intermediate Teff	***8.27***	**8.36**	**102**	***53.78***	**54.93**	**121**	***6.4***	**6.64**	**117**
	(±14%)	**(±14%)**	**(±16%)**	***(±38%)***	**(±32%)**	**(±54%)**	***(±36%)***	**(±32%)**	**(±46%)**
Low Teff	***6.67***	**7.38**	**110**	***128.53***	**49.02**	**38**	***19.15***	**6.61**	**35**
	(±11%)	**(±22%)**	**(±16%)**	***(±22%)***	**(±66%)**	**(±68%)**	***(±15%)***	**(±62%)**	**(±67%)**

	Si:C 0.14		$T_{effSi:C}$ %	Si:N 0.94		$T_{effSi:N}$ %	Si:P 15		$T_{effSi:P}$ %
	34 m	149 m		*34 m*	149 m		*34 m*	149 m	
High Teff	***0.50***	**0.63**	**121**	***3.71***	**5.37**	**137**	***31.45***	**39.00**	**138**
	(±52%)	**(±57%)**	**(±24%)**	***(±46%)***	**(±59%)**	**(±37%)**	***(±60%)***	**(±45%)**	**(±44%)**
Intermediate Teff	***0.40***	**0.44**	**110**	***3.36***	**3.79**	**113**	***22.04***	**24.63**	**131**
	(±50%)	**(±54%)**	**(±10%)**	***(±54%)***	**(±65%)**	**(±18%)**	***(±60%)***	**(±58%)**	**(±47%)**
Low Teff	***0.71***	**0.61**	**95**	***4.86***	**5.01**	**112**	***93.42***	**28.87**	**27**
	(±56%)	**(±67%)**	**(±79%)**	***(±51%)***	**(±83%)**	**(±96%)**	***(±51%)***	**(±69%)**	**(±51%)**

c)	$\delta^{13}C$ ‰		T_{eff13C} %	$\delta^{15}N$ ‰		T_{eff15N} %	$CaCO_3$ mgCa.m^{-2}.d^{-1}		$T_{effCaCO3}$ %
	34 m	149 m		*34 m*	149 m		*34 m*	149 m	
High Teff	***-21.24***	**-19.85**	**93**	***6.71***	**7.54**	**113**	***10.21***	**6.9**	**127**
	(±5%)	**(±6%)**	**(±4%)**	***(±13%)***	**(±23%)**	**(±23%)**	***(±132%)***	**(±79%)**	**(±70%)**
Intermediate Teff	***-21.18***	**-19.93**	**94**	***6.4***	**9.04**	**156**	***14.52***	**3.62**	**30**
	(±3%)	**(±3%)**	**(±2%)**	***(±31%)***	**(±19%)**	**(±40%)**	***(±50%)***	**(±52%)**	**(±65%)**
Low Teff	***-19.47***	**-18.86**	**97**	***7.42***	**7.68**	**107**	***107.21***	**1.76**	**7**
	(±3%)	**(±8%)**	**(±6%)**	***(±20%)***	**(±9%)**	**(±22%)**	***(±131%)***	**(±88%)**	**(±170%)**

Table 3

Figures captions

Figure 1: ***Study area, OMZ O_2 conditions and design of the mooring.***
a) Map of the Eastern South Pacific Oxygen Minimum Zone (in red with $[O_2]_{minimal}$<20 µmol.kg^{-1} from WOA2013 climatology). This map includes the location of the AMOP mooring (white cross, 77.40°W - 12.02°S) off Peru.
b) Vertical distribution of the oxygen concentration at the mooring location (from WOA2013 climatology with the two sediment traps location in black square).
c) Design of the fixed mooring line including two sediment traps, PPS3 with two inclinometers at 34 m near the oxycline and at 149 m in the OMZ core, as well as 5 PTS-O_2 (SBE37-ODO63) at 34, 76, 147 and 160 m, a fluorometer at 31 m, and complementary temperature sensors (SBE56). Sensor depths are indicated to ± 1 m, estimated from sensor pressure and inclinometer data (cf. Methods).

Figure 2: ***Time series in 2013 for POC flux*** *(left handed scale) at 34 m (black bar) and 149 m (white bar)* ***and the corresponding transfer efficiency*** *(T_{eff}; from Eq.1, gray line, right-handed scale), covering $AMOP_{summer}$ (denoted AMOP1, a) and $AMOP_{winter\text{-}spring}$ (denoted AMOP2, b) periods. Error bars correspond to the accuracy of analytical determination for the POC flux and is estimated through a logarithmic expansion of Eq. 1 for T_{eff}. (cf. Methods, Tab. 3a and Tab. S1 for details).*

Figure 3: ***Time series in 2013 of the oxygen concentration*** *(µmol.kg^{-1}) covering $AMOP_{summer}$ (denoted AMOP1) and $AMOP_{winter\text{-}spring}$ (denoted AMOP2) periods, acquired on the mooring location line through oxygen sensors at 34, 76, 147 and 160 m depth with a 15 min acquisition frequency and vertically interpolated (cf. Fig. 1c and Methods). The dashed horizontal white lines indicate the depth of the traps.*

Figure 4: ***Time series documented at the mooring site in 2013 of oxygen concentration and density at the upper trap, of Mixed Layer Depth (MLD) and wind speed in surface, and of POC flux and fluorescence at the upper trap, for each sample****. Left and right panels are for $AMOP_{summer}$, (denoted AMOP1) and $AMOP_{winter\text{-}spring}$ (denoted AMOP2), respectively.*
a-b) Daily oxygen concentration ($\overline{[O_2]}_{1day_15min}$, blue line, and density (red line) calculated from pressure, temperature and salinity data acquired with the PTS sensors (cf. Fig. 1c), at 34 m depth.
c-d) Daily mixed layer depth (purple) and wind velocity (grey) from ASCAT satellite.
e-f) Weekly POC flux at 34 m (black) in mgC.m^{-2}.d^{-1} and daily fluorescence data at 31 m (green) in relative unit.
For more details, cf. Methods.

Figure 5: ***Vertical transfer efficiency for POC (T_{eff}) versus POC flux at the upper trap.***
T_{eff} versus POC flux in mgC.m^{-2}.d^{-1} at 34 m for $AMOP_{winter\text{-}spring}$ (denoted AMOP2) dataset filtering samples with T_{eff}>100% (thus excluding AMOP2-S1, -S3 and –S6, cf. Section "Significance of the transfer efficiency"), with power tendency line (R^2 = 0.88).

Figure 6: ***Average mass flux and particles composition at the upper sediment trap (34m) averaged by main T_{eff} ranges.***
a) Histograms of POC fluxes in mgC.m^{-2}.d^{-1} (cf. Fig. 2) with error bars corresponding to the standard deviation.
b) Sector diagrams of particles composition (mol%) in terms of Particulate Organic Carbon (POC), Particulate Organic Nitrogen (PON), Particulate Organic Phosphorus (POP) and Biogenic Silica (BSi). The values indicated in % correspond to the abundance of one element relative to the sum of the four other elements analyzed here for the OM. For more details, cf. Tables S1 and S2.
Note that due to its specific OM quality at 34 m, AMOP2-S4 sample has been extracted from the intermediate T_{eff} range and represented separately.

Figure 7: ***Mean transfer efficiency for the main components of the particles fluxes*** *(related to POC, PON, POP, BSi, $CaCO_3$, and to particulate $\delta^{13}C$ and $\delta^{15}N$),* ***as a function of the three main T_{eff} ranges*** *defined from POC fluxes. The transfer efficiencies for PON (T_{effPON}), POP (T_{effPOP}), bSi (T_{effBSi}), $CaCO_3$ ($T_{effCaCO3}$), $\delta^{13}C$ (T_{eff13C}) and $\delta^{15}N$ (T_{eff15N}) are derived from Eq.1, as for Teff. Error bars represent the associated Standard Deviation of the elemental transfer for the considered $T_{eff.}$ ranges (More details in Tab. 3).*

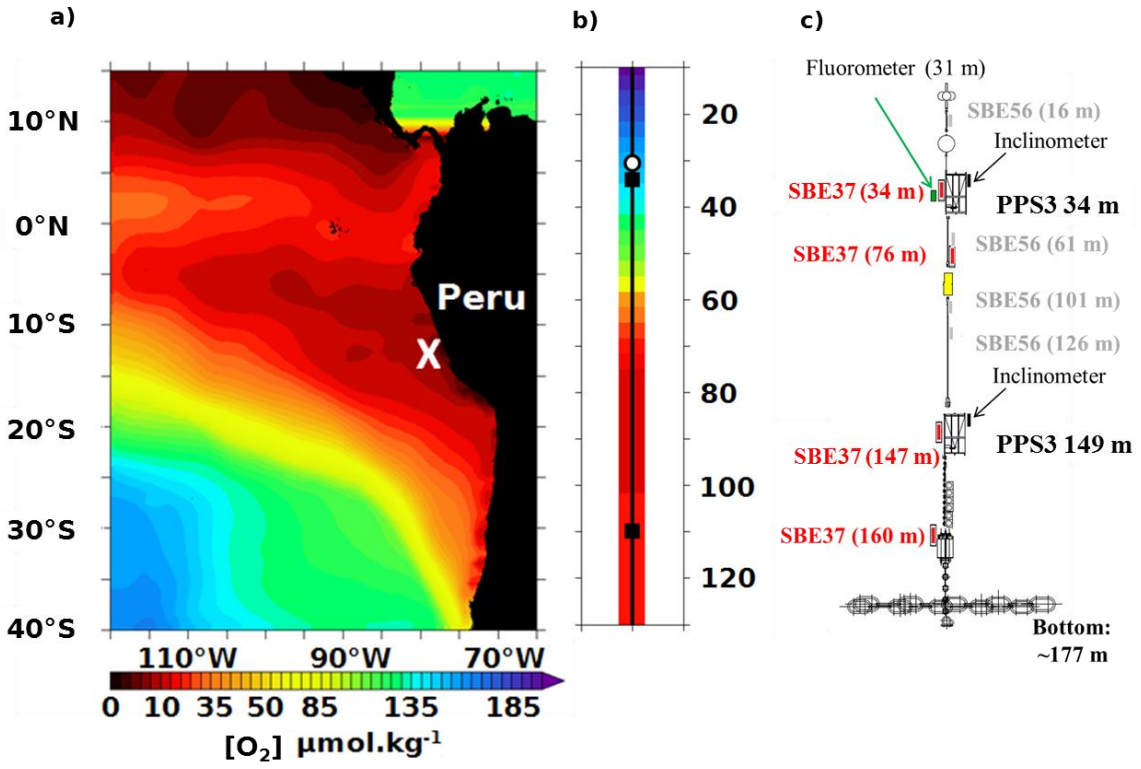
a)
b)
c)
10°N
0°N
10°S
20°S
30°S
40°S
110°W
90°W
70°W
Peru
X
0 10 35 50 85 135 185
[O2] µmol.kg-1
20
40
60
80
100
120
Fluorometer (31 m)
SBE56 (16 m)
Inclinometer
SBE37 (34 m)
PPS3 34 m
SBE37 (76 m)
SBE56 (61 m)
SBE56 (101 m)
SBE56 (126 m)
Inclinometer
PPS3 149 m
SBE37 (147 m)
SBE37 (160 m)
Bottom:
~177 m

Figure 1

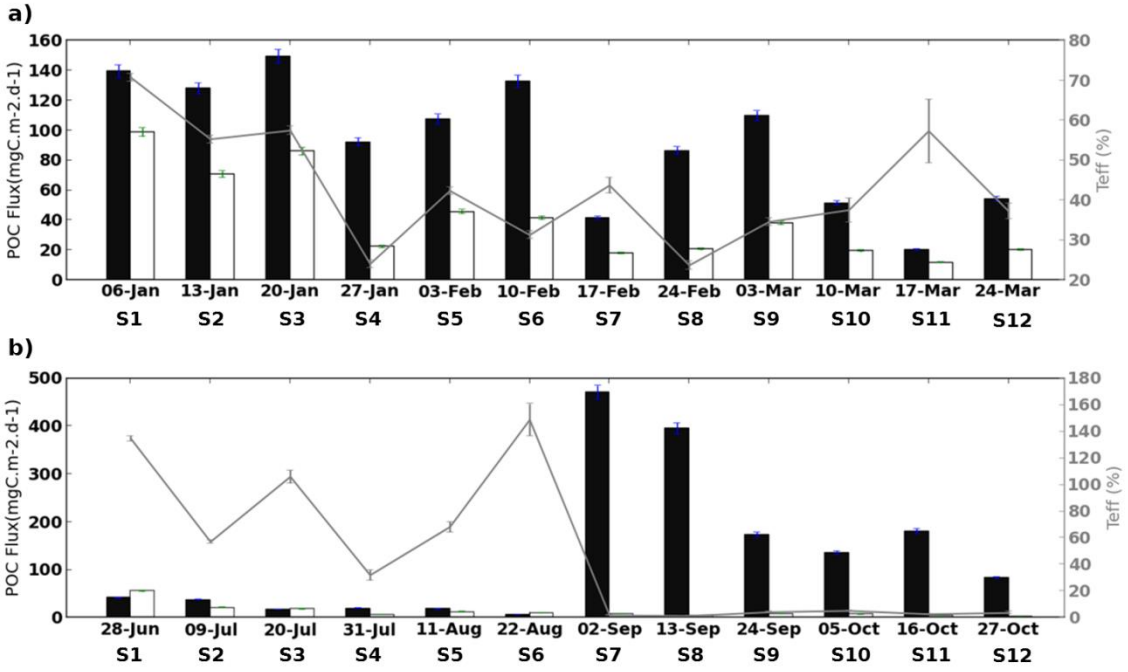
a)
POC Flux(mgC.m-2.d-1)
Teff (%)
06-Jan
13-Jan
20-Jan
27-Jan
03-Feb
10-Feb
17-Feb
24-Feb
03-Mar
10-Mar
17-Mar
24-Mar
S1
S2
S3
S4
S5
S6
S7
S8
S9
S10
S11
S12
b)
POC Flux(mgC.m-2.d-1)
Teff (%)
28-Jun
09-Jul
20-Jul
31-Jul
11-Aug
22-Aug
02-Sep
13-Sep
24-Sep
05-Oct
16-Oct
27-Oct
S1
S2
S3
S4
S5
S6
S7
S8
S9
S10
S11
S12

Figure 2

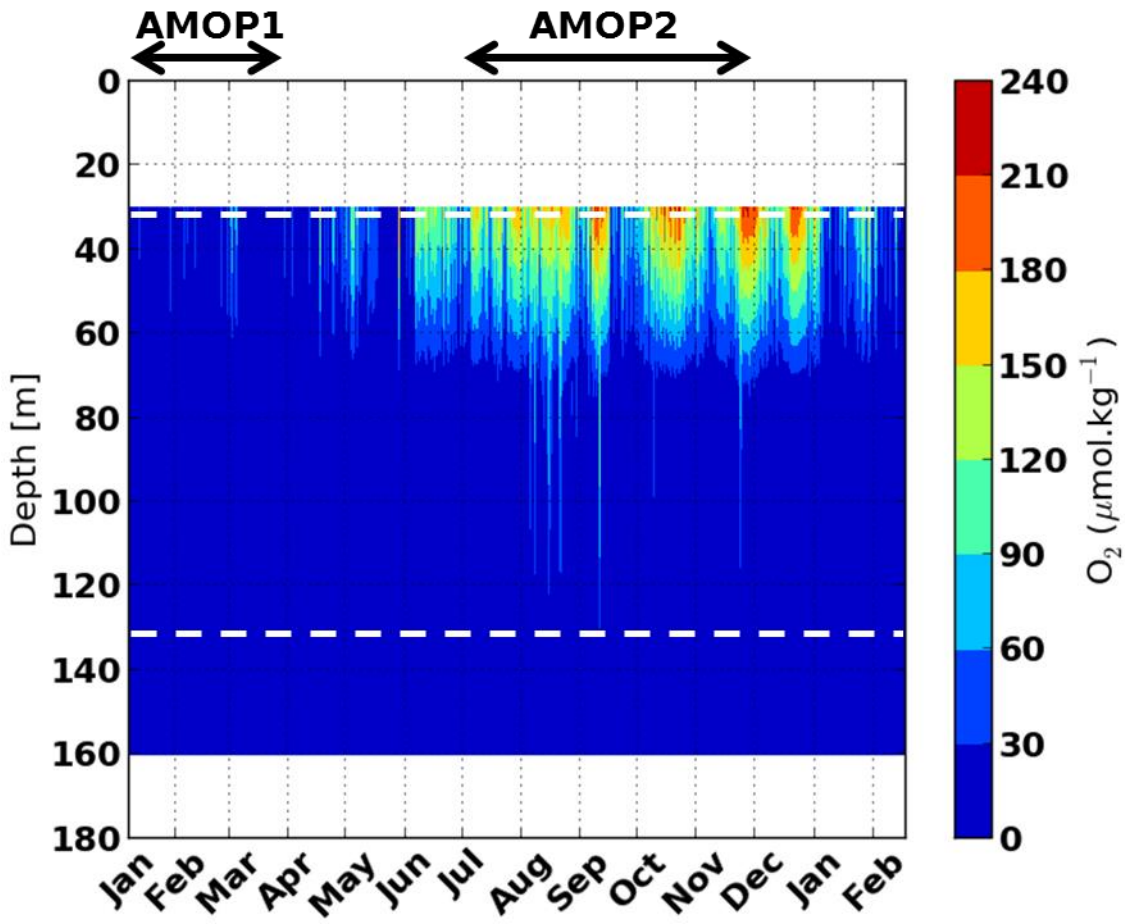
AMOP1
AMOP2
Depth [m]
0
20
40
60
80
100
120
140
160
180
Jan
Feb
Mar
Apr
May
Jun
Jul
Aug
Sep
Oct
Nov
Dec
Jan
Feb
240
210
180
150
120
90
60
30
0
O_2 (μmol.kg^{-1})

Figure 3

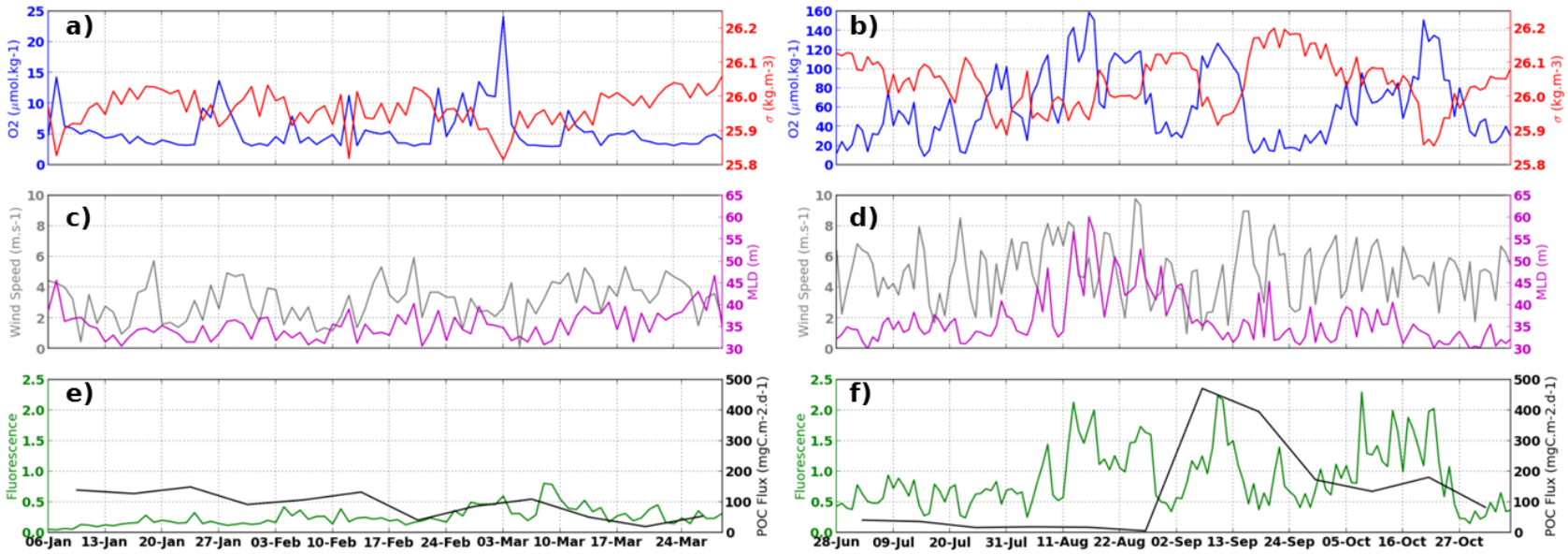
a)
b)
c)
d)
e)
f)
O2 (µmol.kg-1)
σ (kg.m-3)
Wind Speed (m.s-1)
MLD (m)
Fluorescence
POC Flux (mgC.m-2.d-1)
06-Jan 13-Jan 20-Jan 27-Jan 03-Feb 10-Feb 17-Feb 24-Feb 03-Mar 10-Mar 17-Mar 24-Mar
28-Jun 09-Jul 20-Jul 31-Jul 11-Aug 22-Aug 02-Sep 13-Sep 24-Sep 05-Oct 16-Oct 27-Oct

Figure 4

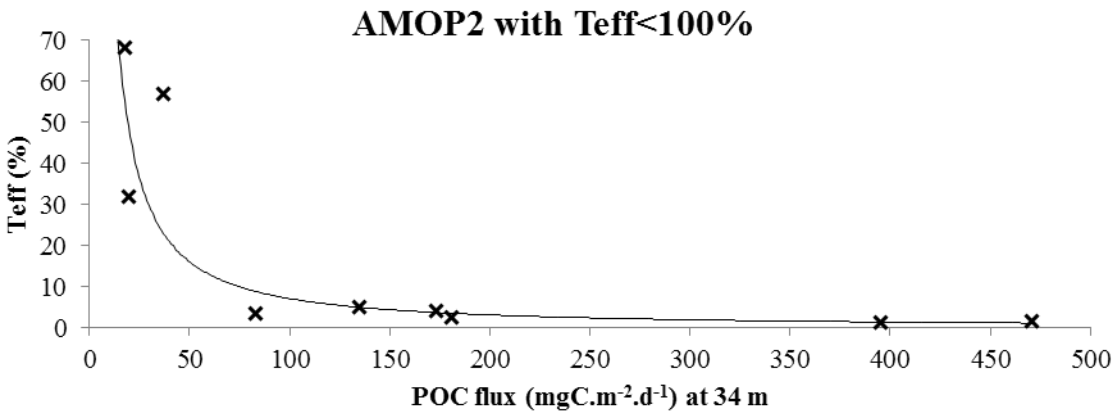
AMOP2 with Teff<100%
Teff (%)
70
60
50
40
30
20
10
0
0
50
100
150
200
250
300
350
400
450
500
POC flux (mgC.m-2.d-1) at 34 m

Figure 5

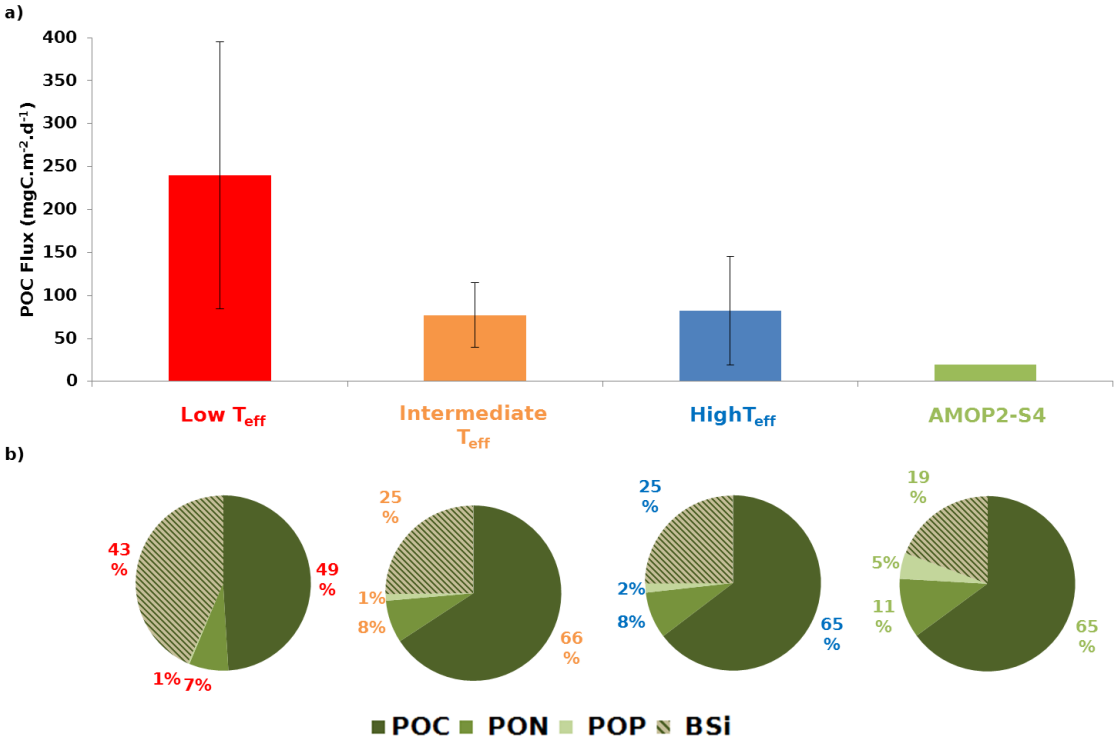
a)
POC Flux (mgC.m-2.d-1)
400
350
300
250
200
150
100
50
0
Low Teff
Intermediate Teff
HighTeff
AMOP2-S4
b)
43 %
49 %
1%
7%
25 %
1%
8%
66 %
25 %
2%
8%
65 %
19 %
5%
11 %
65 %
POC
PON
POP
BSi

Figure 6

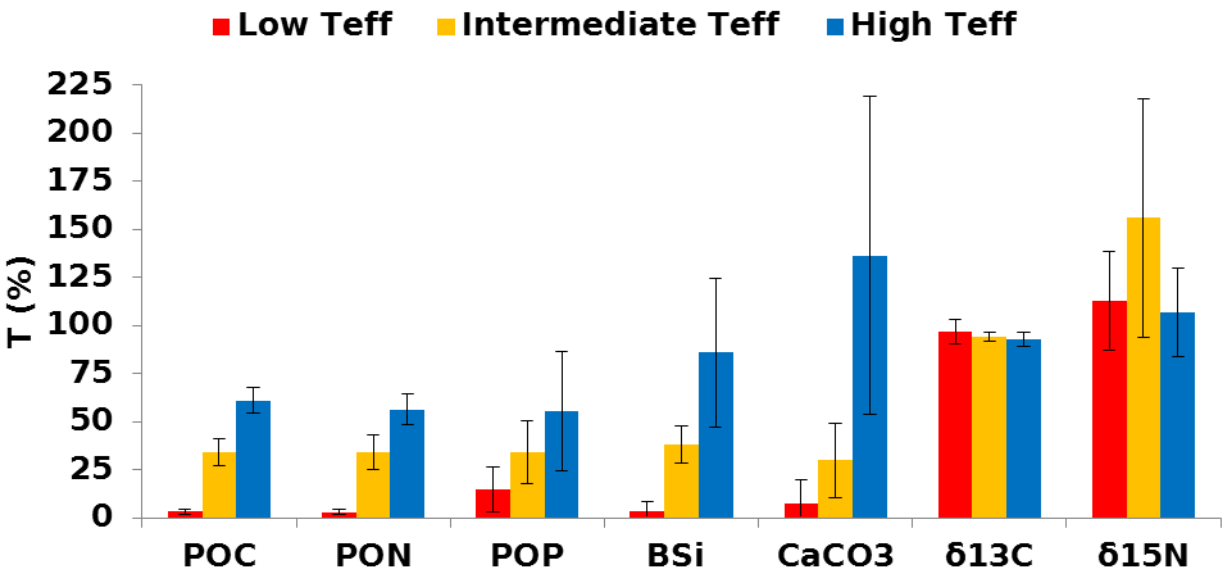
Low Teff
Intermediate Teff
High Teff
T (%)
225
200
175
150
125
100
75
50
25
0
POC
PON
POP
BSi
CaCO3
δ13C
δ15N

Figure 7